Report
P-19-18
December 2019

Äspö Hard Rock Laboratory

Concrete and Clay

Retrieval and analysis of experiment package #20

Per Mårtensson
Mariusz Kalinowski

SVENSK KÄRNBRÄNSLEHANTERING AB

SWEDISH NUCLEAR FUEL
AND WASTE MANAGEMENT CO

Box 3091, SE-169 03 Solna
Phone +46 8 459 84 00
skb.se

SVENSK KÄRNBRÄNSLEHANTERING

ISSN 1651-4416
SKB P-19-18
ID 1692411

December 2019

Äspö Hard Rock Laboratory

Concrete and Clay

Retrieval and analysis of experiment package # 20

Per Mårtensson, Svensk Kärnbränslehantering AB

Mariusz Kalinowski, CBI Betonginstitutet

Keywords: Concrete, Clay, Bentonite, Cement, Waste.

Summary

In 2014, a total of 5 experiment packages were installed within the project Concrete and Clay in TAS06 in the Äspö hard rock laboratory. Each package consisted of 30 blocks made of any of Asha, MX-80, Febex or Ibeco RWC bentonite. In each block, 4 small specimens made of standard or low-pH cement paste were placed, each of which also contained a powder of a metal (Fe, Mo, Ni, Cr) or a metal chloride (CsCl, $SrCl_2$, $EuCl_3$) considered representative of metals which can be found in low- and intermediate-level waste.

During November 2017 experiment package # 20 was retrieved and specimens prepared for analysis. (This series of experiments were numbered from 16-20 as the lower numbers were used for other experiments within this project). This package constitutes a test package for method of retrieval and design of analysis program prior to the retrieval and analyses of the remaining packages which will be undertaken within in a few years' time.

The retrieval was carried out by over-coring the entire package according procedures previously used for retrieval of experiments within e.g. the ABM project. However, over-coring was preceded by an attempt to lift the package after removal of the sand installed in the slit between the package and the wall of the installation hole. However, the attempt failed due to the unexpected large radial swelling of the bentonite blocks.

During the initial part of the retrieval it was noticed that the bolts that secured the lid of the package to its main body had been sheared and that the lid had detached from the main body of the package. This caused extensive swelling of the top bentonite blocks and also to unexpected movements of the cement specimens in the top blocks. For this reason, the 3 top blocks were discarded.

The analyses carried out were focused on interface reactions between cement and bentonite as well as on to what degree the elements that were added to the cement specimens had diffused into the bentonite.

The analyses showed that only very small amounts of the elements mixed into the cement specimens had diffused into the bentonite. The only element for which diffusion was clearly detected was Cs for which a clear diffusion profile extending to a maximum of close to 40 mm into the bentonite was noticed. For the other elements, the concentrations in the bentonite were close to the methods' limit of detection or differed only marginally from the bentonites' original composition.

Interfacial reactions between standard cement paste and bentonite were manifested by distinct diffusion profiles of Ca, Mg and C in the bentonite close to the interface and in many samples a whitish crust was found in the bentonite right at the interface. Taken together the results indicate that the whitish crust consisted of $CaCO_3$ and $MgCO_3$. The effect of diffusion was less apparent on the cement side of the interface. Interface reactions between bentonite and specimens made from low-pH cement were significantly less apparent than between bentonite and specimens made from standard cement paste.

Sammanfattning

Under år 2014 installerades totalt 5 stycken experimentpaket inom projekt Concrete and Clay i TAS06 i Äspölaboratoriets underjordsdel. Varje experimentpaket utgjordes av 30 stycken bentonitblock tillverkade av någon av totalt fyra olika typer av bentonit (Asha, MX-80, Febex och Ibeco RWC). I varje bentonitblock hade även små kutsar bestående av antingen standard cement eller låg-pH cement alternativt en cylinder bestående av kolstål eller rostfritt stål placerats. Varje cementkuts innehöll utöver cementpasta även ett metallpulver (Fe, Mo, Cr, Ni) eller en metallklorid (CsCl, $SrCl_2$, $EuCl_3$) vilka ansågs representativa för metaller som förekommer i låg- och medelaktivt radioaktivt avfall.

Under november månad år 2017 genomfördes återtag av experimentpaket #20, alltså ett av de totalt 5 bentonitpaketen. (Dessa experiment numrerades från 16-20 då lägre nummer användes för andra experiment inom detta projekt). Detta paket utgör testpaket för utveckling av metod för återtag och utformning av analysprogram inför framtida återtag och analyser av de återstående experimentpaketen.

Återtaget genomfördes genom överborrning av hela paketet enligt metod tidigare använd vid återtag av exempelvis experiment i ABM-projektet. Detta föregicks dock av ett försök att lyfta paketet efter rensning av den sandfyllda spalten mellan detta och hålväggen. Försöket misslyckades dock, bland annat på grund av att bentoniten svällt radiellt och därför satt mycket hårt fast i hålet.

Under inledningen av återtaget noterades att bentonitens svälltryck skjuvat av de bultar som höll fast locket på experimentpaketet. Detta hade lett till omfattande svällning av de översta bentonitblocken samt även till att de inplacerade cementkutsarna flyttats från sina ursprungliga positioner. Av denna anledning kasserades de 3 översta blocken.

Analyserna omfattade dels studier av i vilken omfattning de metaller och metalklorider som blandats in i cementkutsarna frigjorts och transporterats ut i bentoniten men även av studier av interaktioner mellan cement och bentonit i gränsytan mellan dessa material.

Analyserna visade att endast mycket små mängder av de inblandade elementen hade diffunderat in i bentoniten. Tydligast diffusion uppvisades av Cs vilken hade diffunderat in upp till närmare 40 mm i ett par av bentonitblocken. För övriga element låg halterna i bentoniten i närheten av metodens detektionsgräns alternativt skiljde sig endast marginellt från bentonitens ursprungssammansättning. Någon mätbar skillnad mellan indiffusion från standardcement och låg-pH-cement kunde inte noteras.

Studier av gränsyteinteraktioner mellan cementkutsarna och bentoniten visade på tydlig indiffusion av Ca, Mg och C från standardcement till bentonit och tydliga diffusionsprofiler av dessa ämnen kunde noteras. I många av proverna noterades även att ett vitaktigt skikt bildats på bentoniten i gränsytan. Sammanvägt med resultaten från EDS-analyserna antyder detta att skiktet består av $CaCO_3$ och $MgCO_3$. I de fall då cementkutsen bestod av låg-pH-cement var indiffusionen av dessa ämnen betydligt mer begränsad och i vissa fall ej detekterbar.

Contents

1 Introduction

1.1 Background

Low- and intermediate level radioactive waste, LILW, is today deposited in the final repository for short-lived low- and intermediate level radioactive waste, SFR, or stored temporarily while waiting for the final repository for long-lived low- and intermediate level radioactive waste, SFL, to be completed and taken into operation.

The LILW consists of a complex mixture of different types of materials including both organic as well as inorganic materials, including large amounts of metals. Prior to disposal the waste is placed in various types of containers which are filled with a mixture of waste and conditioning material, e.g. cement grout or bitumen. Finally, the containers are placed in the repository in which different types of cement-based materials and bentonite are used or are planned for use in the engineered barriers.

In SFR which has been in operation for more than 25 years, concrete and other cement based materials are extensively used in the engineered barrier system, either alone or in combination with bentonite as in the Silo (SKB 2015). In SFR a majority of the waste is conditioned in a cement matrix but some is instead conditioned in bitumen. A certain fraction of the ion exchange resins deposited in the waste vault for concrete tanks, 1BTF and 2BTF is simply just dewatered and placed in concrete tanks without any additional conditioning material.

For SFL which is currently planned to be taken into operation in the year 2045 the SFL concept study finalised in 2013 (Elfwing et al. 2013) suggested that the core components as well as the PWR reactor pressure vessels from the nuclear power plants should be disposed of in a waste vault in which the engineered barrier system is based on the use of concrete alone. The legacy waste currently stored at the Studsvik site and which comprises a complex mixture of different materials and nuclides was suggested to be disposed of inside a concrete structure which is surrounded on all sides by a thick layer of bentonite constituting the main barrier in this waste vault.

Once the repositories have been filled with waste, the rock vaults and transport tunnels will be backfilled with different types of materials, e.g. crushed rock or bentonite. Also large plugs will be constructed to limit water transport in the tunnels and rock vaults. Once the drainage pumps have been turned off, water will slowly fill the repository, saturating the voids and pore systems of the porous materials.

During the long periods of time covered by the safety analyses interactions between the groundwater and species dissolved in the groundwater and the materials in the repositories will occur. These interactions will cause changes in the physical and chemical properties of the barrier materials as well as degradation of the waste leading to the formation of species that may further affect the properties of the materials in the engineered barriers. Besides affecting the properties of the materials in the engineered barriers, low molecular organic degradation products may also affect the retaining capacity of the barrier systems through complexation with the radionuclides.

Concrete degradation in a post closure perspective has been extensively studied by many different organisations over the years with Höglund (2014) probably presenting the broadest study, covering not only chemical degradation but also the impact of mechanical processes such as corrosion of reinforcement bars, gas formation, freezing etc. Further, Idiart and Shafei (2019) have studied the development of the chemical and physical properties of concrete over a one million year perspective whereas Idiart and Laviña (2019) investigated the influence of alternative cement compositions.

Interactions between bentonite and concrete have been examined in several previous studies by means of computer modelling; see e.g. Höglund (2001), Gaucher et al. (2005) and Cronstrand (2007, 2016) of which Gaucher et al. (2005) presents the most extensive study.

As a complement to these modelling studies in which also interactions with the waste is included the project Concrete and Clay was initiated. See also Mårtensson (2015).

1.2 Project objectives

The objective of this project is to increase the understanding of the processes that occur when the waste, conditioning grout and the material used in the engineered barriers interact under the influence of an anoxic groundwater. The following issues have been identified as being of particular interest in the work presented in this report:

- Corrosion of metals (Here represented by Cr, Fe, Mo, Ni.) in a cementitious environment and diffusion of the corrosion products in the cement matrix and surrounding bentonite.
- Dissolution of metal salts (Here represented by CsCl, $SrCl_2$, $EuCl_3$.) in a cementitious environment and diffusion of the metal ions in the cement matrix and surrounding bentonite.
- Cement/bentonite interactions with main focus on inter diffusion of the parent elements between these two material types. Here also differences in diffusion profiles involving interactions between bentonite and standard cement paste and low-pH cement paste respectively were of special interest.

1.3 Experimental concept

During the time period 2010–2014 a total of 9 packages comprising concrete cylinders or bentonite blocks each containing different types of waste form materials representative for low- and intermediate-level radioactive waste were installed in 3 different sections in the Äspö Hard Rock Laboratory according to the following:

- **Concrete and clay phase 1 comprising field scale concrete experiments**: 2 packages, each containing 3 concrete cylinders with material samples (both organic materials and metals) representative of LILW..
- **Concrete and clay phase 2 comprising field scale concrete experiments**: 1 package containing 3 concrete cylinders with material samples (both organic and metals) representative of LILW and one package containing 3 concrete cylinders without material specimens.
- **Concrete and clay phase 3 comprising field scale bentonite experiments**: 5 packages, each containing 30 bentonite blocks were installed in TAS06. Each bentonite block contains 4 small cylinders made of standard or low-pH cement paste or a solid cylindrical specimen made of carbon steel or stainless steel. The vast majority of the small cylinders also contain a metal powder (Fe, Ni, Cr. Mo) or a powder of a metal chloride (CsCl, $SrCl_2$. $EuCl_3$) representative of low and intermediate level waste or container material but a few are used as blanks without any additional material.

The experiments are illustrated in Figure 1-1 and 1-2 and fully described in Mårtensson (2015).

As a complement to the field scale experiments also smaller laboratory scale experiments were carried out. The laboratory scale experiments comprised a total of 20 stainless steel containers which all were filled with about 1 000 ml of Äspö ground water, about 50 grams of crushed hardened cement paste and material specimens of the same type as used in the field scale concrete experiments.

The purpose of the laboratory scale experiments was to provide an indication on the extent of degradation of the waste over time. By analysing the water in the containers a suitable time for the retrieval of the first field scale concrete experiments could be obtained.

Figure 1-1. *The five bentonite packages in TAS06 after completion of the installation.*

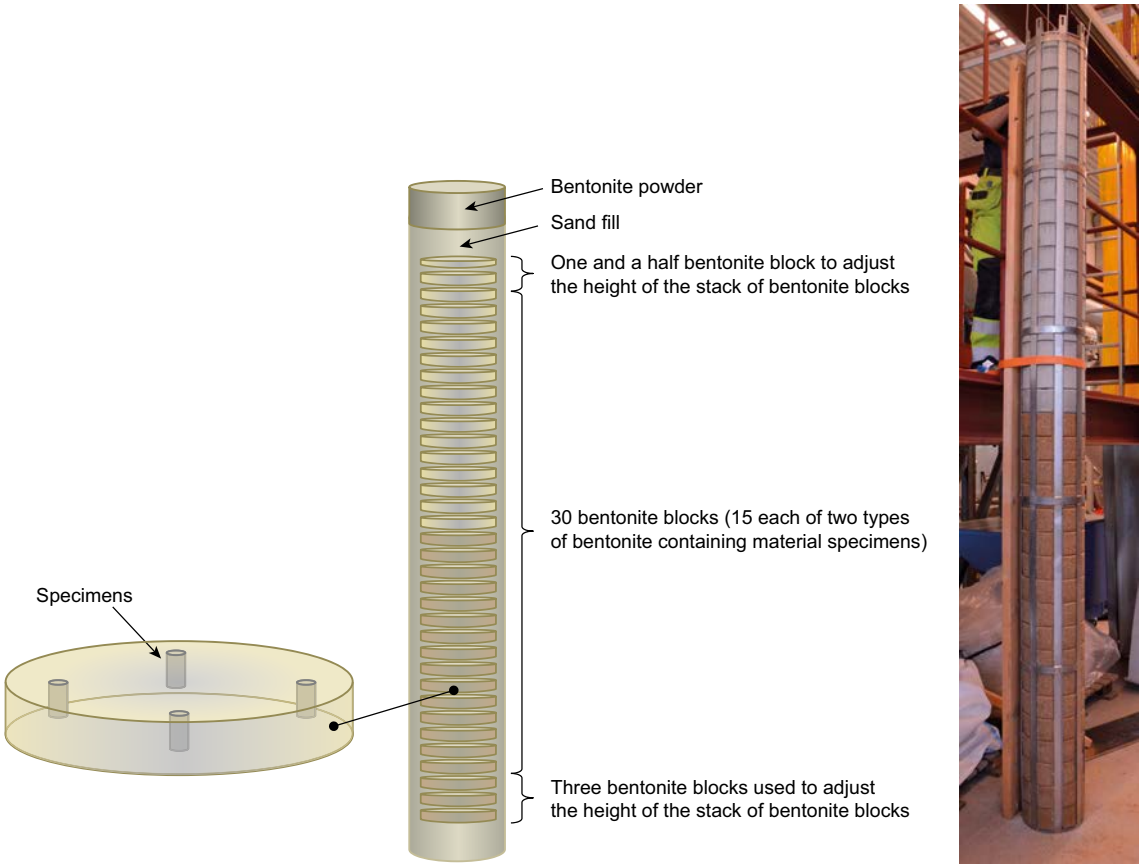

Figure 1-2. *Schematic illustration of a bentonite experiment package and a photograph of the actual package before installation.*

1.4 Description of Concrete and Clay experiment #20

Concrete and Clay experiment # 20 comprises 30 bentonite blocks made from Febex, Asha, MX-80 and Ibeco RWC bentonite. For a short description of the different bentonite types; please refer to Svensson et al. (2011). Each block also contains 4 different specimens made from standard cement paste or low-pH cement paste or a small cylinder made from carbon steel or stainless steel. A majority of the cement specimens also contain a powder of one of the following materials; Fe, Mo, Cr, Ni, CsCl, $SrCl_2$ or $EuCl_3$ but a few are used as references and do not contain any additional material.

From this description it can easily be understood that all combinations of types of bentonite, cement paste and material powder are not present in this experiment. Instead this experiment covers a few selected combinations of which initially only a selected number was analysed in order to obtain the desired information discussed in the following section.

1.5 Purpose and scope of the work presented in this report

The purpose of concrete and Clay experiment # 20 is primarily to serve as a means of developing methods for retrieval and analyses. Further, the purpose is also to obtain a first indication on the extent of the interactions between the cement specimens and the bentonite blocks for planning of future retrieval of the remaining packages within this project.

The work presented in this report covers the following aspects:

- Method for retrieval. Attempt to lift the package without prior over coring
- Methods for segmentation of the bentonite blocks
- Method for sample preparation prior to analysis
- Method for analysis of trace elements in water saturated bentonite
- Plan for future retrieval and analyses: Obtaining a first indication regarding the rate of reactions for setting up a time plan for future retrievals and methods of analyses.

2 Retrieval of the experiment package

2.1 Retrieval without prior over coring

2.1.1 Original plan

In connection with the installation work, the approximately 7 mm wide slit between the bentonite package and the wall of the installation hole wall was filled with sand. The purpose of this sand was to counteract the bentonite swelling and to evenly distribute the water around the entire bentonite package. Prior to retrieval, the sand would be removed and the package released. After this the package was expected to be lifted without the need for the usual over coring, i.e. hammer drilling in the surrounding bedrock.

2.1.2 Implementation and result

As a first step the bolts holding the beams securing the lid were unscrewed and the concrete lid removed, Figure 2-1.

This was followed by removal of the top sand by means of a powerful vacuum cleaner and digging out of the bentonite seal thus exposing the titanium lid of the experiment package, Figure 2-2.

At this stage it was noticed that the titanium lid was oblique and that the flat irons in which the lid was originally bolted could not be seen. This was surprising as the lid was originally attached to the flat iron which constituted the cage by means of 8 M8 bolts (Figure 2-3, left image).

Figure 2-1. *The beams have been removed and the lid is lifted. The tubes protruding from the sand provided water for saturation of the bentonite.*

Figure 2-2. *The bentonite on top of the experiment package is removed and the lid is exposed.*

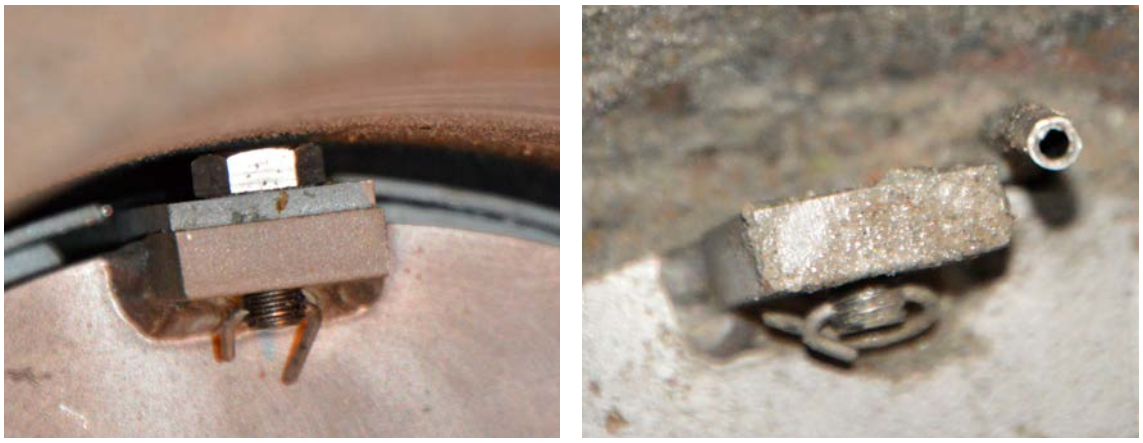

Figure 2-3. *The left image shows how the lid is bolted to one of the flat irons that make up the main body of the titanium cage. In the right image, the bolt has been sheared and the titanium lid moved from its original position.*

However, as indicated in Figure 2-2 (right) and more clearly shown in Figure 2-3 (right), all bolts fastening the lid to the main body of the titanium cage except 2 were sheared due to the bentonite swelling pressure. This allowed the lid to be pushed from its original position and the topmost bentonite blocks to expand more or less freely once the restraining force from the lid was lost. Based on a comparison of images from assemblage of the experiments and images from retrieval it is estimated that that total expansion of the three or four topmost blocks was in the order of 120-150 mm. See also Sections 3.1 and 3.2 and 5.2.2 for further details on the effects of this.

In order to be able to carry out retrieval according to the proposed methodology, the titanium lid was removed and the flat irons exposed. This was done by first removing the lid and then enough bentonite to expose the flat irons. The deletion of parts of these blocks did not affect the blocks containing the small cement specimens as the top 2 blocks and the bottom 3 blocks were only used to adjust the height of the bentonite stack, Figure 1-2.

Once the flat irons had been exposed, lifting eyes were mounted in the holes where the bolts were previously attached, Figure 2-4, and a first attempt to lift the package without any other preparations was carried out. A load cell was mounted between the lifting device and the package and the lift was carried out to a load of approximately 2 000 kg. This can be compared to the weight of the package which was about 500 kg.

The attempt was unsuccessful and the package remained stuck in the hole. Further lifting attempts followed after more thorough removal of sand from the slit. However, all of these were no more successful than the first attempt and finally the strategy was abandoned.

It can be noted here that in spite of the sand in the slit, the swelling pressure of the bentonite had pushed the flat irons of the titanium cage towards the periphery of the installation hole and made removal of the sand very difficult. This meant that the cleansing of the slit in accordance with the intended plan could not be carried out.

Figure 2-4. *Lifting eyelets have been mounted in the flat irons before the first lifting attempt.*

2.2 Over coring followed by retrieval

After the failed attempt discussed in Section 2.1 it was decided to retrieve the package according to normal practice, i.e. through over coring in the surrounding bedrock. Drilling was carried out by means of hammer drilling and a slit was drilled around the entire package in such a way that about 100 mm of rock remained left around the package, Figure 2-5.

Figure 2-5. *Drilling of a slit around the entire package has been completed.*

Also here some problems were encountered due to fracturing of the exposed bedrock between the package and the slit, causing both the package and the drill to jam, Figure 2-6.

In order to be able to release the package, the fractured rock pieces were removed one by one by hand in a rather exhausting process. Finally, after various gymnastics exercises, the package was considered sufficiently clear for a new lift attempt to be motivated, Figure 2-7. During this work, also the lid was again attached to the main body of the package.

A lifting latch with a load cell was mounted in the lids' lifting eye and in the lifting device. The lifting force was slowly increased to approximately 3 500 kg where the package was suddenly released and could be lifted up from the hole intact, Figure 2-8.

After the lift, the package was wrapped in plastic and placed in the transport cradle and transported up to the laboratory for sectioning, packaging and labelling, Figure 2-9.

Figure 2-6. *Fracturing of the exposed rock surrounding the package hampered further drilling as the drill jammed.*

Figure 2-7. *The package is sufficiently cleared to carry out a new lift attempt.*

Figure 2-8. *The package is lifted from the hole.*

Figure 2-9. *The package has been retrieved and wrapped in plastic.*

3 Sectioning, packaging and labelling

3.1 Removal of plastic cover and cutting the titanium cage

The day after the retrieval, the package was opened, the titanium cage cut in half and the bentonite blocks exposed, Figure 3-1.

As shown in Figure 3-2, the top blocks are as a consequence of the problems discussed in Section 2-1 no longer clearly distinguishable but have instead coalesced into a mud-like structure.

Figure 3-1. *The plastic sheet has been removed from the package and the titanium cage cut in half.*

Figure 3-2. *The top part of the package showing how the top blocks have coalesced into a structure with the resemblance of mud rather than clearly distinguishable separate blocks.*

3.2 Sectioning

As a first step, the joints between the individual bentonite blocks were identified and marked. This was rather straight forward as the joints were clearly visible in the entire package, the upper somewhat coalesced blocks surprisingly also included.

After identification of the joints, the top 2 dummy blocks - i.e. the blocks that only were used to adjust the height of the bentonite stack and which not were a part of the experiment - were removed. See also Figure 1-2. To great surprise, cement specimens were found in these blocks, Figure 3-3. These specimens were found close to 10 cm from their original positions and caused great uncertainty. The underlying process that caused the cement specimens to move such great distances as observed here can only be speculated on. However, a plausible explanation is that swelling has been inhomogeneous within the separate blocks with a higher degree of swelling in the interior parts than in the outer for which expansion was restricted by strong adhesion to the rock wall as well as the titanium cage. The net effect of this would be that the specimens moved in relation to the joints between the blocks which were used as points of reference in this work. Due to this swelling and the unclear positions of the specimens in the top blocks, it was instead decided to section the package from the bottom and up as expansion of the lower-most bentonite blocks were not expected to have occurred, Figure 3-4.

When the lower dummy blocks were removed, the bentonite blocks containing the cement specimens could easily be identified and separated from each other by means of a tool for debarking of logs, Figure 3-5.

However, for the top 3 blocks shown in Figure 1-2 – dummy blocks not included - problems with the blocks being coalesced and very wet and therefore much harder to separate from each other were encountered. Instead of the debarking spade also other tools had to be used to separate the blocks from each other. However, during this work it was realised that the cement specimens had moved a significant distance from their original positions. It was also realised that this would have destroyed the original cement-bentonite interfaces and analysis of these specimens would therefore be of no use. For that reason it was decided to discard the upper 3 blocks.

Figure 3-3. *Test cut in the top dummy block showing the unexpected presence of a cement specimen in the middle of the image.*

Figure 3-4. *Removal of the 3 dummy blocks at the bottom of the package. Note how the bentonite swelling pressure has made the thick titanium bottom plate convex. Here the joints between the different blocks are clearly visible.*

Figure 3-5. *One of the lower Asha bentonite blocks.*

3.3 Segmentation, packaging and labelling

After sectioning of the package, the individual bentonite blocks were segmented into 4 equally sized segments each containing a cement or steel specimen using a standard band saw. The shape of the segments is indicated in Figure 3-6. After segmentation, the individual sections were placed in aluminium bags which were vacuum sealed and labelled, Figure 3-6. A list of the specimens is found in Table A1 in Appendix A.

Finally, samples were selected for analysis. A couple of specimens were sent to the laboratory at Äspö for analyses of density and water content, while about 40 samples were sent to an external laboratory for analyses. The remaining specimens were placed on their own pallet and saved for future needs, Figure 3-7.

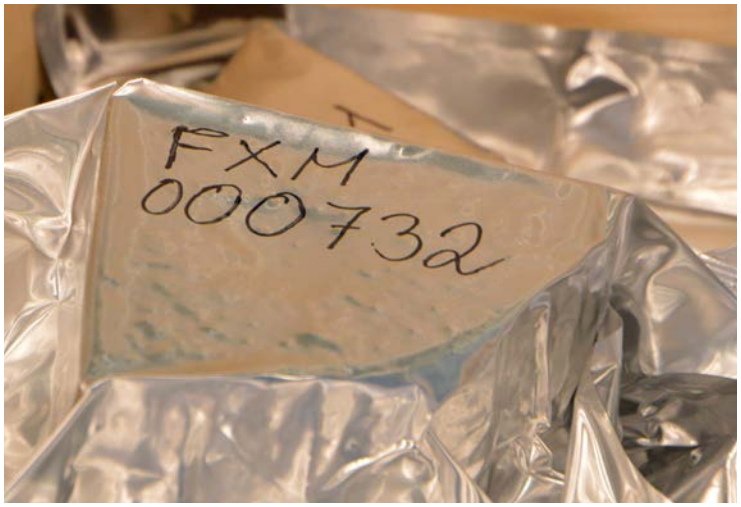

Figure 3-6. *Aluminium bag containing one quarter of a bentonite block after vacuum sealing and labelling.*

Figure 3-7. *Samples after sectioning, packaging and labelling.*

4 Material analyses

As presented in Section 1.2 the main focus in this work was on studies on interface diffusion between cement and bentonite as well as on release and diffusion of elements representative of low- and intermediate level waste which had been added to the cement specimens embedded in the bentonite blocks. For that reason, the method of choice was Scanning Electron Microscopy in combination with Energy Dispersive X-ray Spectroscopy in order for selected area analyses to be possible at a high enough resolution and low enough detection limit.

4.1 Methods

4.1.1 SEM/EDS

Description of the method

Analyses of the chemical composition of the bentonite clay and cement specimens were made by Environmental Scanning Electron Microscopy (E-SEM) equipped with a Back-Scattered Electron detector (BSE) and Energy Dispersive X-ray Spectroscopy (EDS). The acceleration voltage was 20 keV. EDS analyses include elements from atomic number 6, i.e. carbon and heavier. The total pressure in the analysing chamber was 0.59 mbar and vapour of deionized water was used as a pressure stabilizing gas. Typically the analysed areas were 0.5*0.5 mm or 1.0*1.0 mm.

Analyses were made in one or more areas at different distances from the interface between the bentonite clay and the embedded cement specimen. Here, the composition of the bentonite at a distance of about 40 mm from the interface was chosen as the reference composition of the bentonite clay. All the analysed areas were first checked by means of a BSE detector to avoid any contaminated areas.

The results from the EDS analyses were normalized to 100 % by weight. Analysis time was 110-120 live seconds (lsec) at a dead time (DT) of about 40 %. This corresponds to an analysis time of approximately 5 minutes per area. Quantification from EDS spectra was made with peaks for K transitions for elements through atomic number 26 (Fe). For elements with higher atomic numbers, i.e. Sr, Mo, Cs and Eu, the L-transitions were used.

The pre-set SEC factors (Standardless Element Coefficients) of the EDAX software were used to quantify the elements Cr, Sr, Mo, Cs and Eu. Quantification of the other elements, including Fe, was calibrated against a Portland cement paste of known chemical composition (certified reference material from Bureau of Analysed Samples Ltd., Britain). Measurement uncertainty for levels of Fe and Cs is estimated at approximately 10 % of the measurement value i.e. +/- 0.3-0.4 % by weight for Fe and 0.1-0.2 % by weight for Cs. Analysis of the elements Cr, Sr, Mo and Eu is considered qualitative because measured levels are close to the level of the detection limit of the method, i.e. 0.1 % by weight.

The analyses of Sr and Mo were difficult because the spectral L-transitions of the elements overlap stronger K-transitions with the elements Si and S, also found in the bentonite clay. To optimize the treatment of spectra, a careful manual adjustment of the background in energy areas for the said peaks was made. A qualitative analysis of Sr and Mo with EDAX software was combined with ocular review of the shape of the peaks. The detection limit for the elements Sr and Mo is nevertheless considered to be higher than for the other elements in the analysis and is estimated to be roughly 0.2 % by weight.

Sample preparation

The bentonite clay specimens were removed from the bags in which they had been stored and transported and chopped with a chisel immediately before analysis, Figure 4-1. All specimens were moist at the time of analyses.

Specimens of bentonite clay stretching from the cement/bentonite interface into the bentonite to a distance of about 40 mm from the interface were removed using a knife. (Figure 4-2, left image) The dimensions of these specimens were about 10×10-15×15 mm (Figure 4-2, right image).

Figure 4-1. *Chopping of the bentonite block exposed the cement/bentonite interface*

Figure 4-2. *Specimens prepared for analysis.*

4.1.2 Density

The sample bulk density (D_b = total mass/total volume) was determined by weighing the material in air and submerged in paraffin oil. The bulk density was thereafter calculated according to:

$$D_b = \frac{\mathrm{m} \times D_{paraffin}}{m_{paraffin}}$$

where m is the mass of the specimen, $D_{paraffin}$ is the density of the paraffin oil, and $m_{paraffin}$ is the mass of displaced paraffin oil, measured as the weight difference between the specimen in air and in paraffin oil. All density results are compiled in Table 5-3.

4.1.3 Water-to-solid ratio

The water-to-solid mass ratio (w) was determined by drying the material in a laboratory oven at 105°C for 24 h, and the water-to-solid mass ratio was calculated according to:

$$w = \frac{\mathrm{m} - \mathrm{m}_d}{\mathrm{m}_d}$$

where m_d is the mass of the dry sample. All water-to-solid mass ratio results are compiled in Table 5-3.

5 Results

5.1 Bentonite composition

The composition of the bentonite was determined as the average of the values from the EDS measurements at a distance of 40 mm from the interface between the cement specimen and the bentonite for each of the 4 types of bentonite. The results are presented in Table 5-1.

Table 5-1. Average composition of the four different types of bentonite used in this study at a distance of about 40 mm from the cement/bentonite interface.

Element	Asha	Febex	Ibeco RWC	MX-80
C	2.07	1.89	3.74	4.36
O	48.89	50.72	49.92	49.05
Na	0.46	0.35	0.31	0.51
Mg	1.65	2.84	2.09	1.57
Al	13.02	11.66	12.27	12.19
Si	21.60	26.42	24.13	26.79
S	0.09	0.11	0.17	0.33
Cl	0.10	0.11	0.13	0.11
K	0.08	0.63	0.50	0.25
Ca	1.40	1.42	2.19	1.10
Ti	0.46	0.20	0.47	0.09
Fe	10.16	3.59	4.08	3.62
Mo	0.06	0.37	0.02	0
Sr		0		0
Cs		0	0	0
Eu		0.01	0	0.03
Ca:Si	0.065	0.053	0.091	0.041
Mg:Si	0.076	0.11	0.087	0.059

5.2 Density and water content

5.2.1 Installed density

Table 5-2 shows the density, water content and degree of saturation of the different types of bentonite prior to installation (Mårtensson 2015). The “Installed dry density” presented in the rightmost column in Table 5-2 is an estimate of the dry density of a bentonite block which has been allowed to swell radially out to the wall of the installation hole. No swelling of the block along the axis of the hole has been assumed in these calculations.

Table 5-2. Measured and calculated data for the different types of bentonite blocks prior to installation.

Type of bentonite	Average weight (kg)	Average volume (dm^3)	Water content at pressing (%)	Compacted dry density (kg/m^3)	Installed dry density (kg/m^3)
Asha	12.45	6.0	20.1	1 630	1 390
Febex	12.03	6.04	18.5	1 620	1 380
Ibeco RWC	11.70	6.05	18.6	1 570	1 350
MX-80	11.9	6.08	19.2	1 580	1 360

5.2.2 Density after retrieval

Table 5-3 shows the density and water to solid ratio of the 4 different types of bentonite after retrieval. The measurements clearly show a lower dry density and higher water to solid ratio in the upper parts of the package than in the lower parts. This is a clear effect of the more or less free swelling of the upper blocks as discussed in Section 3.1.

Table 5-3. Density and water to solid ratio of the bentonite after retrieval.

Type of Bentonite	Specimen	Depth below rock floor (mm)	Density (kg/m^3)	Dry density (kg/m^3)	Water to solid ratio	Degree of saturation (%)*
Febex	FXM000691	1100	1811.2	1303.3	0.39	97.0
Febex	FXM000694	1200	1899.3	1422.1	0.34	99.4
Febex	FXM000710	1600	1958.1	1521.0	0.29	98.4
Ibeco RWC	FXM000722	1900	1942.6	1484.5	0.31	99.4
MX-80	FXM000743	2400	1986.4	1553.8	0.28	100.1
MX-80	FXM000776	3200	2004.1	1579.6	0.27	100.4
Asha	FXM000786	3500	2048.2	1604.7	0.28	100.6
Asha	FXM000802	3900	2032.9	1584.5	0.27	100.1

* Degree of saturation has been calculated using grain density data from Table 6-1 in Svensson et al. (2011).

5.3 Diffusion of trace elements in the bentonite blocks

5.3.1 Asha bentonite

Caesium

Diffusion of Cs in Asha bentonite was studied using specimens FXM000795. In this specimen the small cylinder containing the CsCl powder was made of standard cement paste.

The results of the analysis are presented in Figure 5-1. A comparison with the background level of Cs in Asha bentonite indicate that extensive Cs diffusion has occurred and increased levels of Cs are found up to about 35-40 mm from the cement-bentonite interface. Cs diffusion is also evident from the distinct Cs profile in the material.

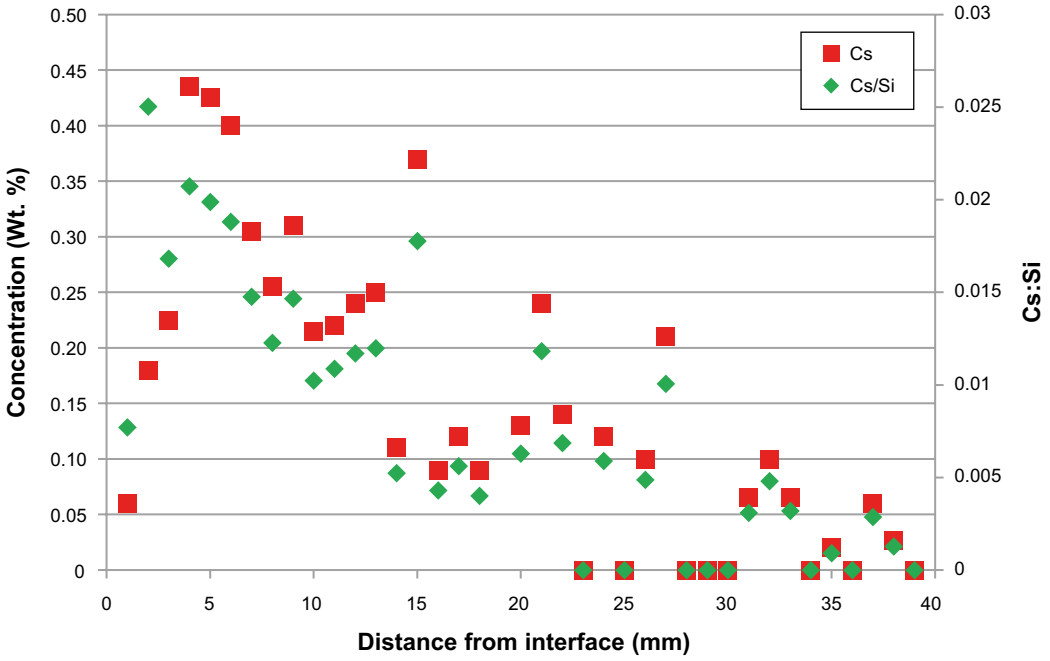

Figure 5-1. *Concentration profile of caesium in Asha bentonite, specimen FXM000795.*

Strontium

Diffusion of Sr in Asha bentonite was not studied in this work.

Europium

Diffusion of Eu in Asha bentonite was studied using specimens FXM000793 and FXM000794. In these specimens the small cylinders containing the $EuCl_3$ powder were made of standard cement paste.

The Eu concentrations found in the Asha bentonite, Figures 5-2 and 5-3 were below or very close to the detection limit for the method used (0.1 %) and also in the same range as the background level in Asha bentonite, Table 5-1. Based on this it can be concluded that Eu release from the cement specimens has been minute even though it cannot be proven with certainty that no release has occurred.

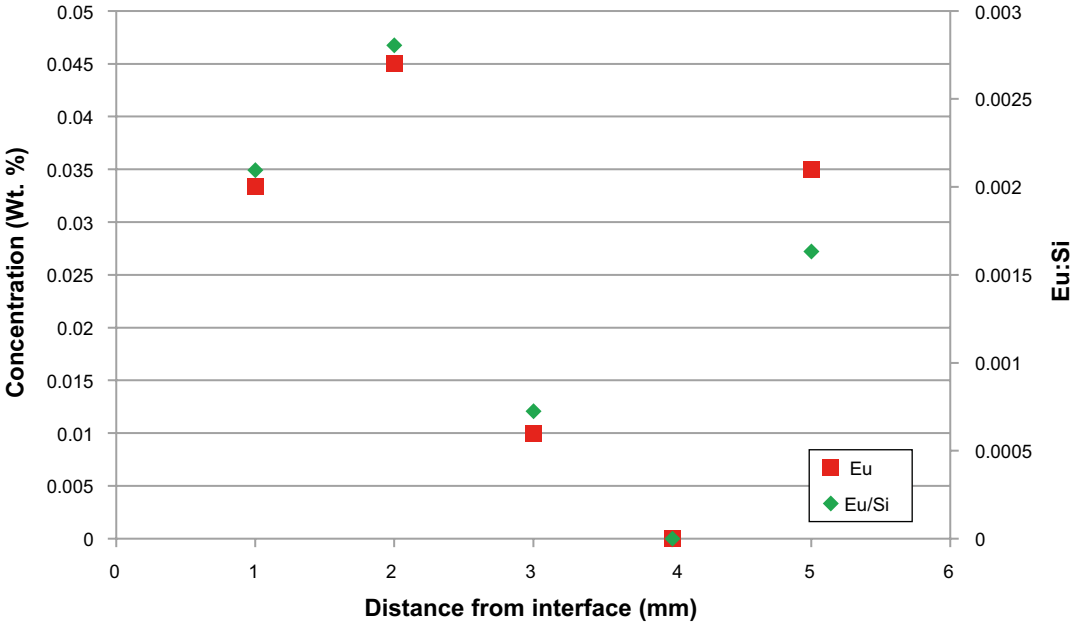

Figure 5-2. *Concentration profile of europium in Asha bentonite, specimen FXM000793.*

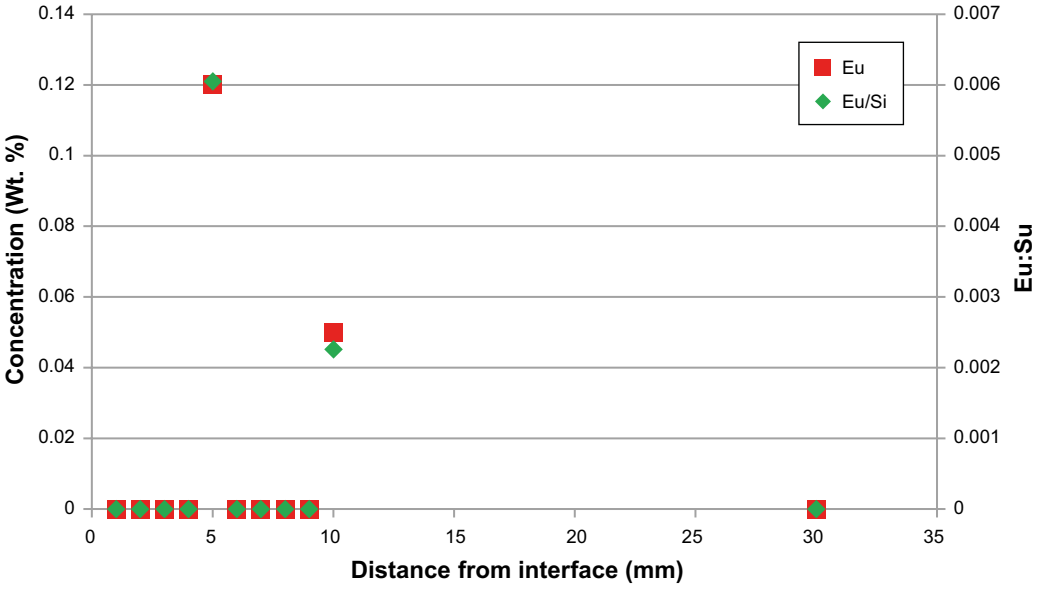

Figure 5-3. *Concentration profile of europium in Asha bentonite, specimen FXM000794.*

Iron

Diffusion of Fe in Asha bentonite was studied using specimens FXM000778 and FXM000798. In FXM000778 the small cylinder containing the Fe powder was made of standard cement paste whereas in FWM000798 it was made of low-pH cement paste.

The Fe concentrations found in the Asha bentonite were significant but still not exceeding the background levels of Fe in Asha bentonite, Table 5-1. For the standard cement specimen (Figure 5-4) the Fe concentration was much lower close to the interface than further into the bentonite but for the low-pH cement specimen the variations were much smaller, Figure 5-5. However, for both specimens the Fe:Si ratio was rather constant throughout the specimen indicating that the large variations observed for the standard cement specimen is a consequence of an increased Ca concentration close to the interface for this specimen; see also Section 6-1. The very high levels of Fe in Asha bentonite makes identification of small variations caused by Fe diffusion from the cement specimen difficult and it is therefore not possible to conclude that Fe diffusion has occurred even though the levels are high.

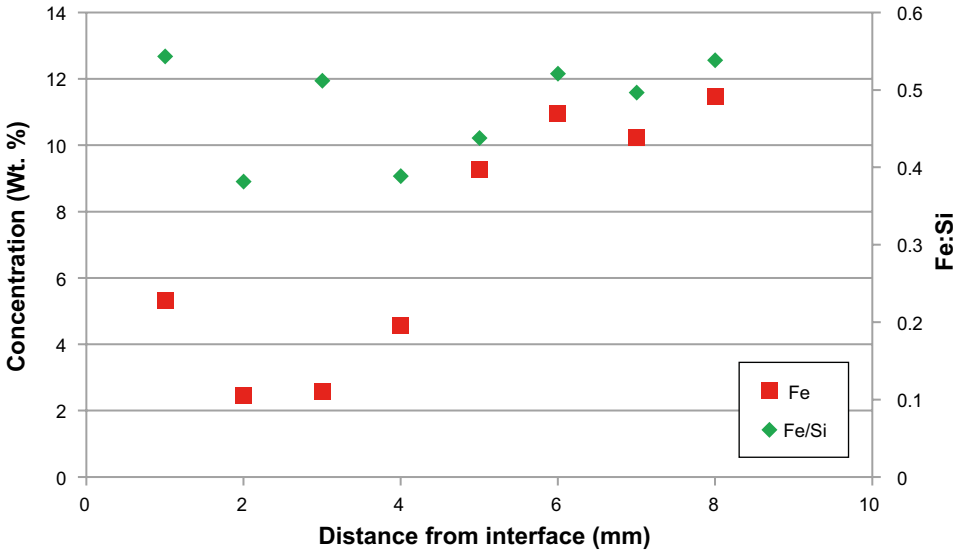

Figure 5-4. *Concentration profile of iron in Asha bentonite, specimen FXM000778.*

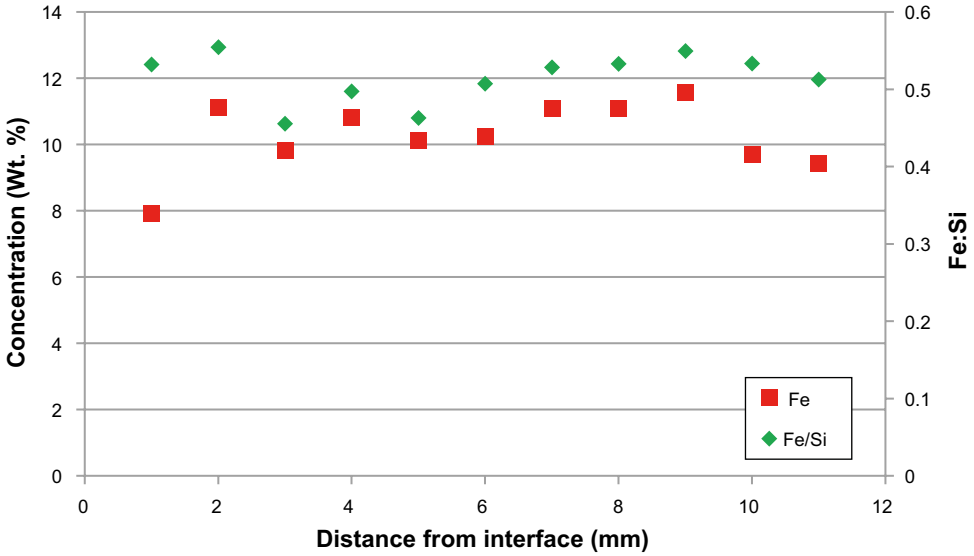

Figure 5-5. *Concentration profile of iron paste in Asha bentonite, specimen FXM000798.*

Nickel

Diffusion of Ni in Asha bentonite was not studied in this work.

Chromium

Diffusion of Cr in Asha bentonite was not studied in this work.

Molybdenum

Diffusion of Mo in Asha bentonite was studied using specimens FXM000780 and FXM000799. In FXM000780 the small cylinder containing the Mo powder was made of standard cement paste whereas in FXM000799 it was made of low-pH cement paste.

The Mo concentrations found in the Asha bentonite, Figures 5-6 and 5-7, were below or very close to the detection limit for the method used (0.1 %) and also on the same levels as the background level of Mo in Asha bentonite, Table 5-1. Based on this it can be concluded that Mo release from the cement specimens has been minute even though it cannot be proven with certainty that no release has occurred.

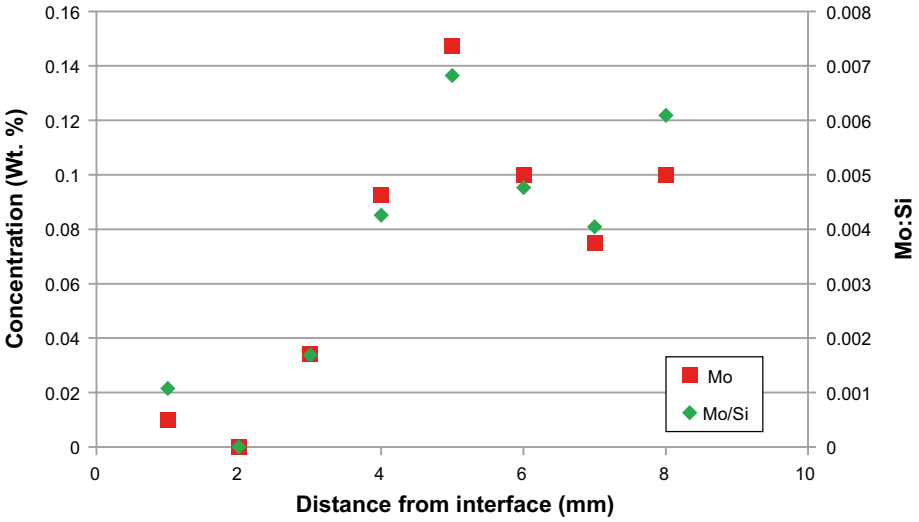

Figure 5-6. *Concentration profile of molybdenum in Asha bentonite, specimen FXM000780.*

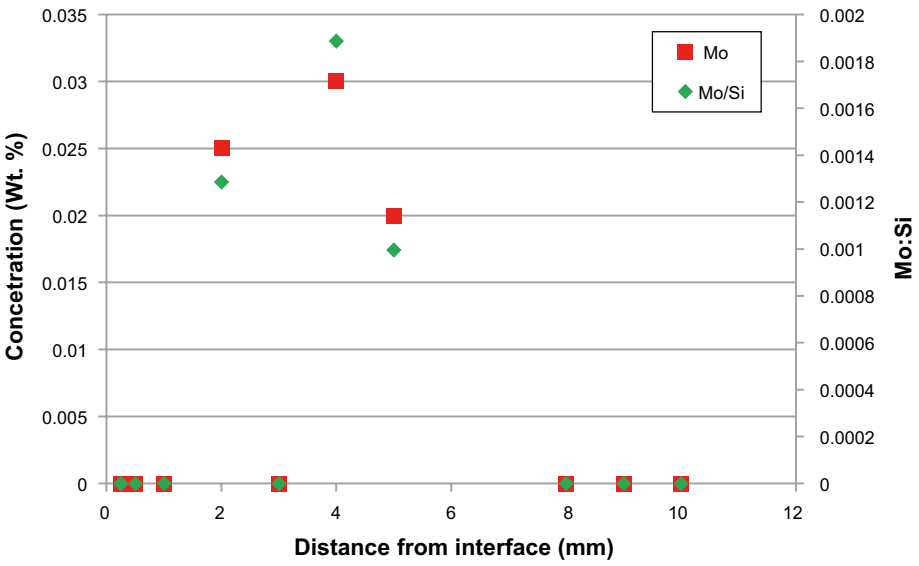

Figure 5-7. *Concentration profile of molybdenum in Asha bentonite, Specimen FXM000799.*

5.3.2 Febex bentonite

Caesium

Diffusion of Cs in Febex bentonite was studied using specimens FXM000703 and FXM000704. In these specimens the small cylinders containing the CsCl powder were made of standard cement paste.

From Figures 5-8 and 5-9 a clear increase in the Cs concentration close to the cement/bentonite interface is found. The levels of Cs are well above the detection limit for the method and also well above the background level of Cs in Febex bentonite, Table 5-1. It can thus be concluded that Cs has diffused out of the cement specimens and into the bentonite.

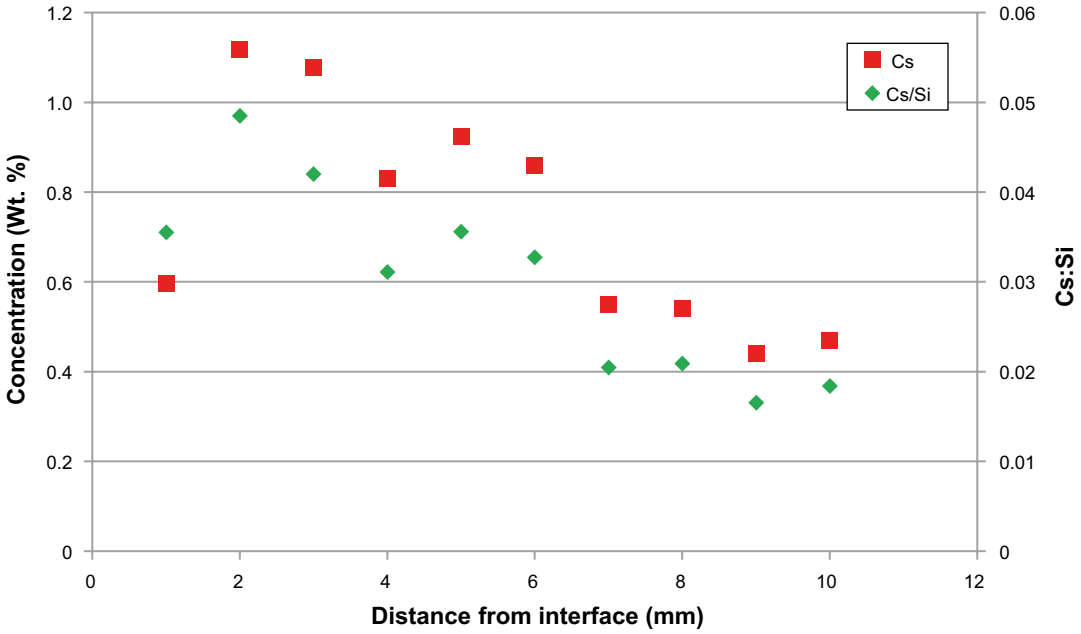

Figure 5-8. *Concentration profile of caesium in Febex bentonite, specimen FXM000704.*

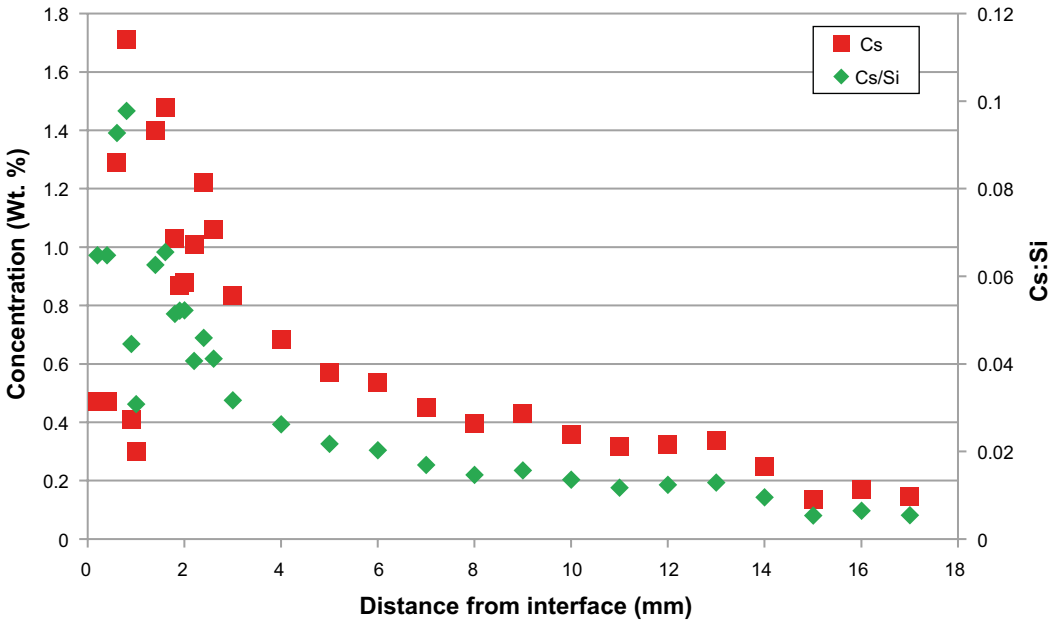

Figure 5-9. *Concentration profile of caesium in Febex bentonite, specimen FXM000703.*

Strontium

Diffusion of Sr in Febex bentonite was studied using specimen FXM000697. In this specimen the small cylinder containing the $SrCl_2$ was made of standard cement paste. Here, the analyses could not detect any Sr at all in the bentonite.

Europium

Diffusion of Eu in Febex bentonite was studied using specimens FXM000701 and FXM000702. In these specimens the small cylinders containing the $EuCl_3$ powder were made of standard cement paste.

The Eu concentrations found in the Febex bentonite, Figures 5-10 and 5-11, were below the detection limit for the method used (0.1%) and on the same level as the background level of Eu in Febex bentonite (Table 5-1). Based on this it can be concluded that Eu release from the cement specimens has been minute even though it cannot be proven with certainty that no release has occurred.

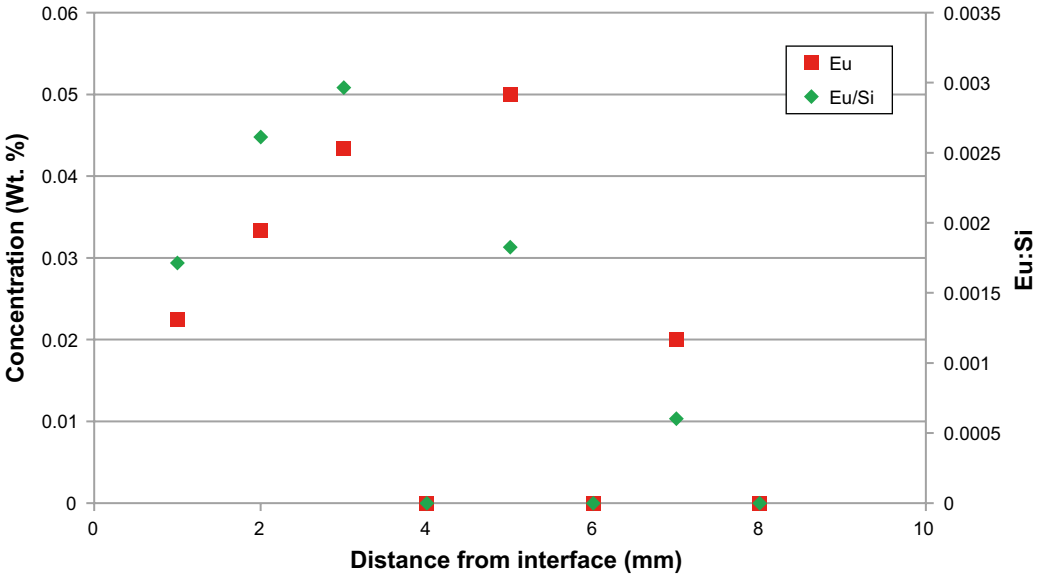

Figure 5-10. *Concentration profile of europium in Febex bentonite, specimen FXM000702.*

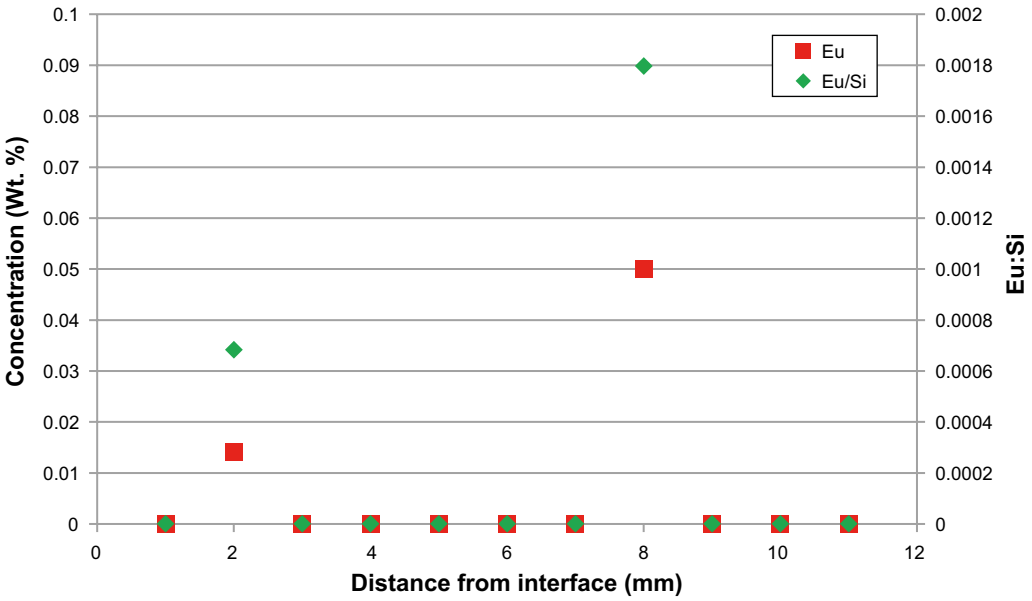

Figure 5-11. *Concentration profile of europium in Febex bentonite, specimen FXM000701.*

Iron

Diffusion of Fe in Febex bentonite was studied using specimen FXM000705. In this specimen the small cylinder containing the Fe powder was made of low-pH cement paste.

The Fe concentrations found in the Febex bentonite were significant but with only small variations between the cement-bentonite interface and areas further into the bentonite, Figure 5-12. The levels found are also in close agreement with the background level of Fe in Febex bentonite, Table 5-1. Based on this it can be concluded that Fe release from the cement specimens has been low even though it cannot be proven with certainty that no release has occurred.

Nickel

Diffusion of Ni in Febex bentonite was not studied in this work.

Chromium diffusion

Diffusion of Cr in Febex bentonite was not studied in this work.

Molybdenum

Diffusion of Mo in Febex bentonite was studied using specimen FXM000708. In this specimen the small cylinder containing the Mo powder was made of low-pH cement paste.

The Mo concentrations found in the Febex bentonite were above the detection limit for the method used but with only small variations between the cement-bentonite interface and areas further into the bentonite, Figure 5-13. The Mo levels detected are very close to the background composition of the Febex bentonite, Table 5-1. Based on this it can be concluded that Mo release from the cement specimens has been low even though it cannot be proven with certainty that no release has occurred.

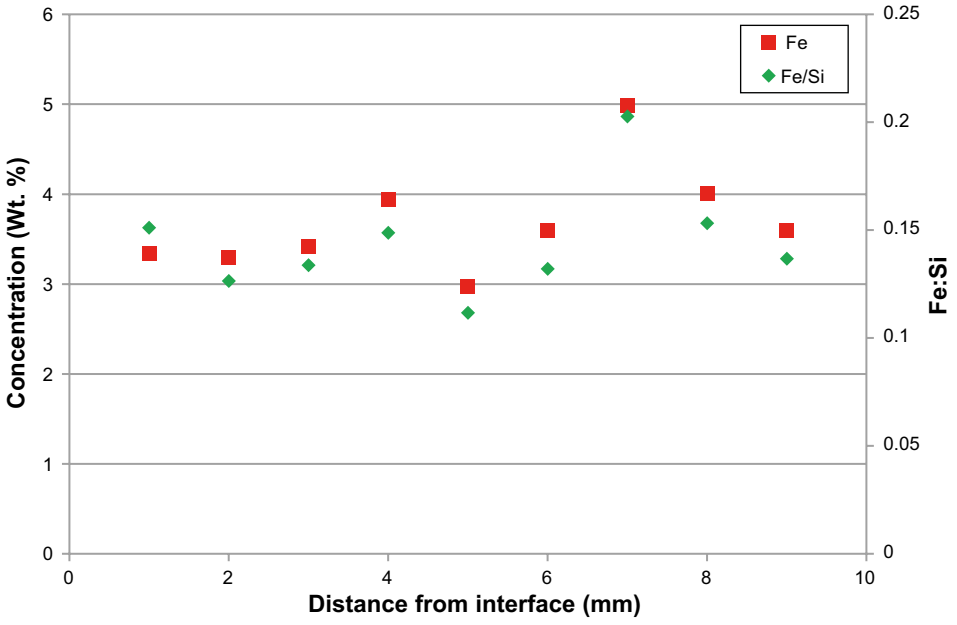

Figure 5-12. *Concentration profile of iron in Febex bentonite, specimen FXM000705.*

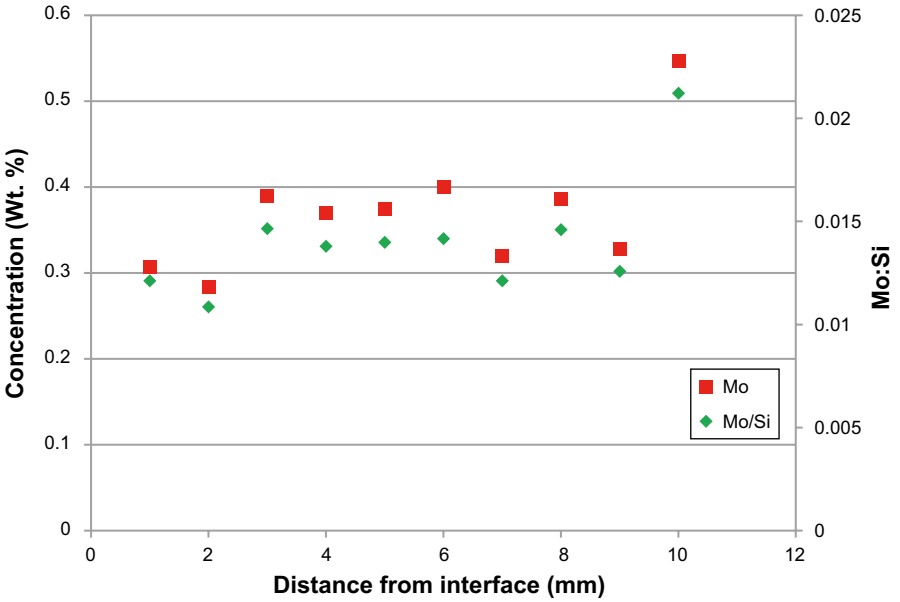

Figure 5-13. *Concentration profile of molybdenum in Febex bentonite, specimen FXM000708.*

5.3.3 Ibeco RWC bentonite

Caesium

Diffusion of Cs in Ibeco RWC bentonite was studied using specimens FXM000731 and FXM000732. In both these specimens the small cylinders containing the CsCl powder were made of standard cement paste.

Figure 5-14 show a clear increase in the Cs concentration close to the cement/bentonite interface. The levels of Cs are well above the detection limit for the method and also well above the background level of Cs in Ibeco RWC bentonite, Table 5-1. It can thus be concluded that Cs has diffused out of the cement specimens and into the bentonite.

The low concentration of Cs found in specimen FXM000731 (Figure 5-15) is a bit puzzling when compared with the results in Figure 5-14. The Cs levels are slightly above the background level of the bentonite (Table 5-1) but with the absence of the clear profile shown in the other specimens. Considering the risk of specimen confusion in any of the many steps involved in the handling of the specimens, the results from this analysis must be evaluated with some scepticism and the results are therefore neglected here.

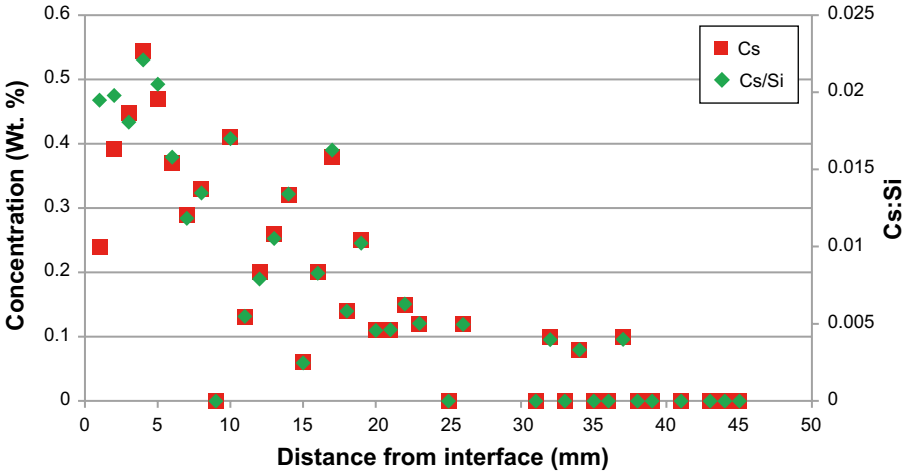

Figure 5-14. *Concentration profile of caesium in Ibeco RWC bentonite, specimen FXM000732.*

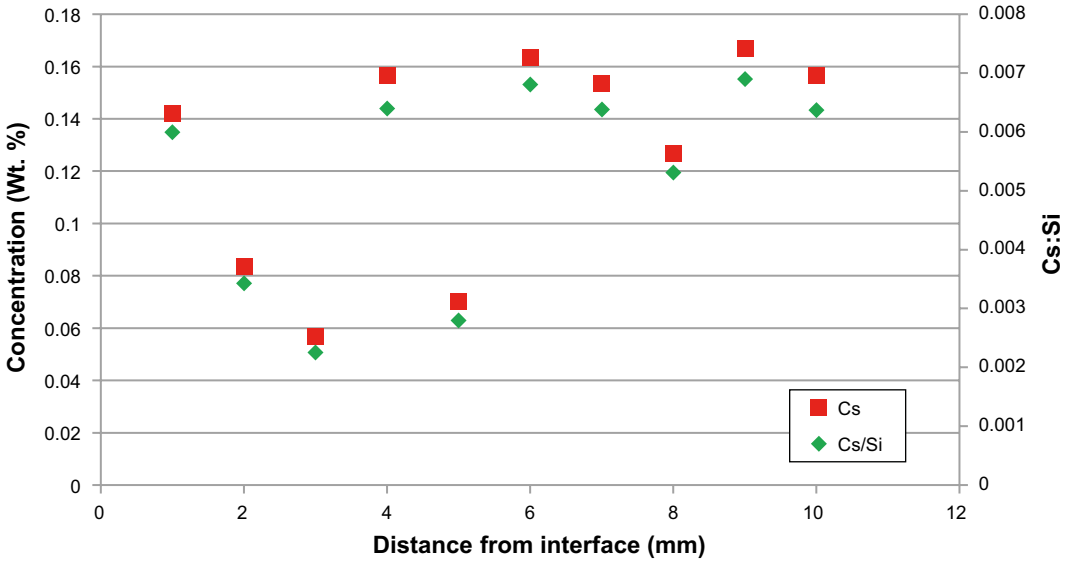

Figure 5-15. *Concentration profile of caesium in Ibeco RWC bentonite, specimen FXM000731.*

Strontium

Diffusion of Sr in Ibeco RWC bentonite was studied using specimen FXM000725. In this specimen the small cylinder containing the $SrCl_2$ powder was made of standard cement paste.

As shown in Figure 5-16, slightly elevated levels of strontium are found close to the cement/bentonite interface. Being so close to the detection limit of the method (0.1 % by weight), this should be regarded as an indication of that some Sr has been released from the cement specimen rather than a quantitative measure. The background level is not reported in Table 5-1 but from Figure 5-16 it should be basically 0.

Europium

Diffusion of Eu in Ibeco RWC bentonite was studied using specimen FXM000730. In this specimen the small cylinder containing the $EuCl_3$ powder was made of standard cement paste.

As shown in Figure 5-17, no Eu was found in the Ibeco RWC bentonite.

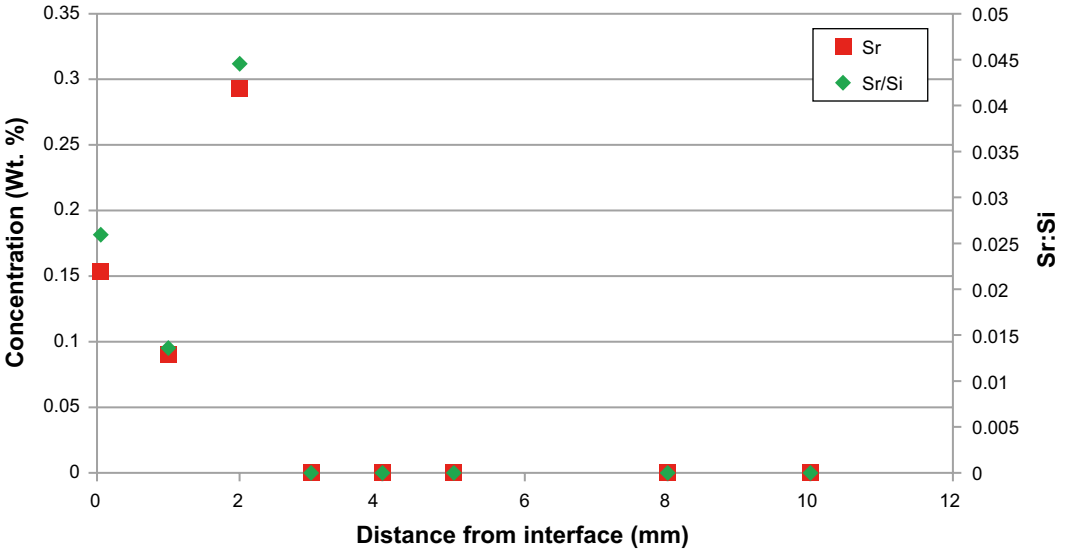

Figure 5-16. *Concentration profile of strontium in Ibeco RWC bentonite, specimen FXM000725.*

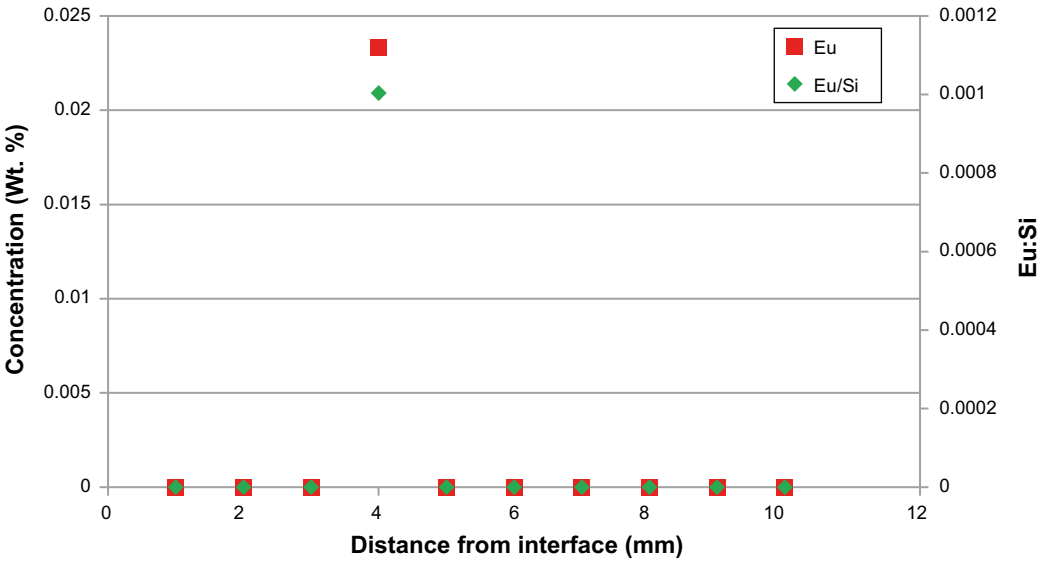

Figure 5-17. *Concentration profile of europium in Ibeco RWC bentonite, specimen FXM000730.*

Iron

Diffusion of Fe in Ibeco RWC bentonite was studied using specimens FXM000714 and FXM000734. In FXM000714 the small cylinder containing the Fe powder was made of standard cement paste whereas in FXM000734 it was made of low-pH cement paste.

The results of the analyses presented in Figure 5-18 and 5-19 do not indicate any in diffusion of Fe into the bentonite. Instead the Fe:Si ratio is approximately the same irrespective of distance from the interface and the levels of Fe are close to the background level for this type of bentonite, Table 5-1.

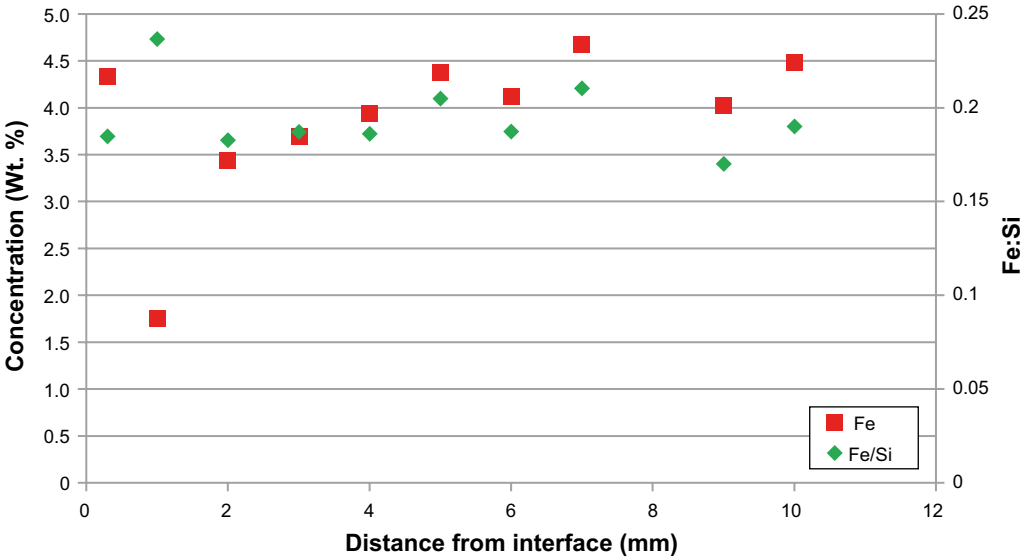

Figure 5-18. *Concentration profile of iron in Ibeco RWC bentonite, specimen FXM000714.*

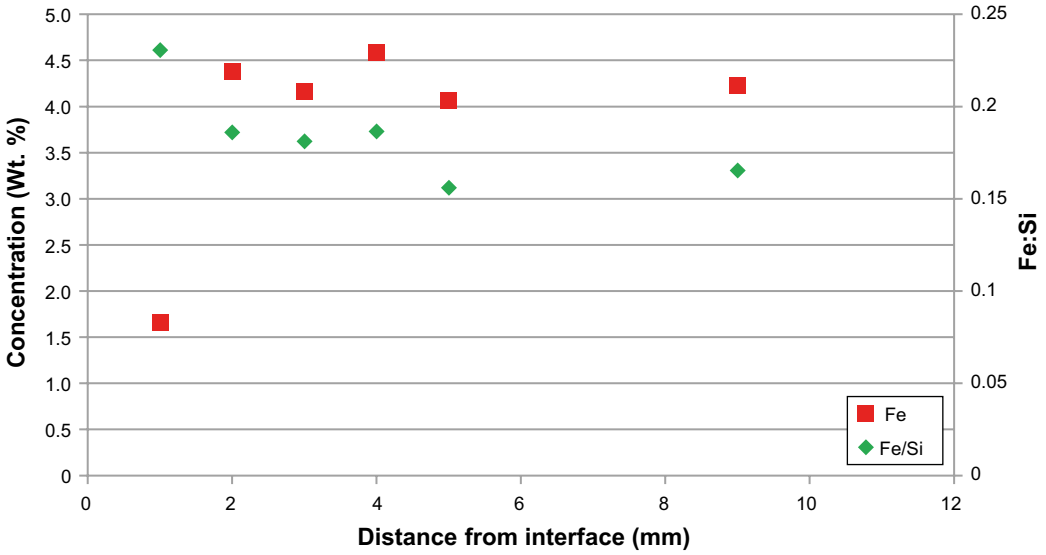

Figure 5-19. Concentration profile of iron in Ibeco RWC bentonite, specimen FXM000734.

Nickel

Diffusion of Ni in Ibeco RWC bentonite was studied using specimen FXM000719 in which Ni was mixed with standard cement paste. Even though at very low levels, the concentration of Ni presents a small gradient from the interface and into the bentonite, Figure 5-20. However, due to that the concentration is so close to the detection limit of the method it cannot be conclusively claimed that this is proof for Ni release from the cement specimen.

Chromium

Diffusion of Cr in Ibeco RWC bentonite was studied using specimen FXM000718 in which Cr was mixed with standard cement paste. The detected levels of Cr are below the detection limit of the method used, Figure 5-21. No Cr has thus been released from the cement specimen.

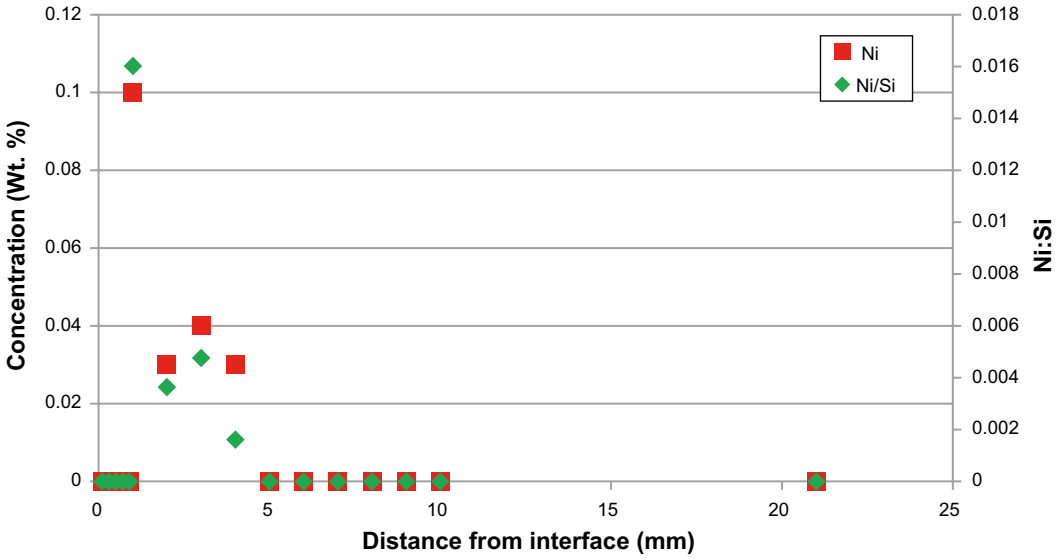

Figure 5-20. Concentration profile of nickel in Ibeco RWC bentonite, Specimen FXM000719.

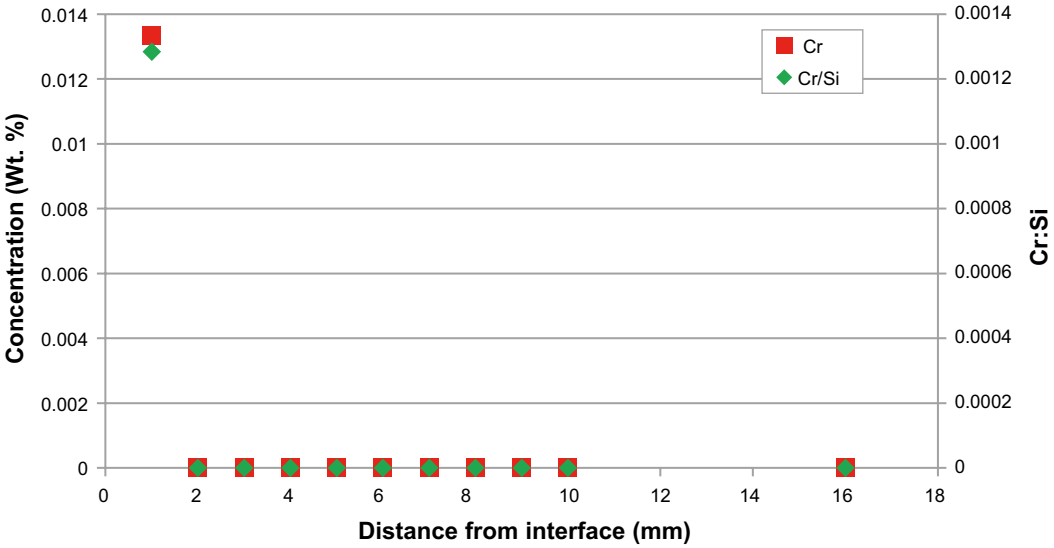

Figure 5-21. *Concentration profile of chromium in Ibeco RWC bentonite, Specimen FXM000718.*

Molybdenum

Diffusion of Mo in Ibeco RWC bentonite was studied using specimens FXM000715 and FXM000736. In FXM000715 the small cylinder containing the Mo powder was made of standard cement paste whereas in FXM000736 it was made of low-pH cement paste.

As shown in Figures 5-22 and 5-23, the levels of molybdenum in the bentonite are very low and close to or below the detection limit for the method even though somewhat above the background level of Mo in this type of bentonite, Table 5-1. Based on this it can be concluded that Mo release from the cement specimens has been minute even though it cannot be proven with certainty that no release has occurred.

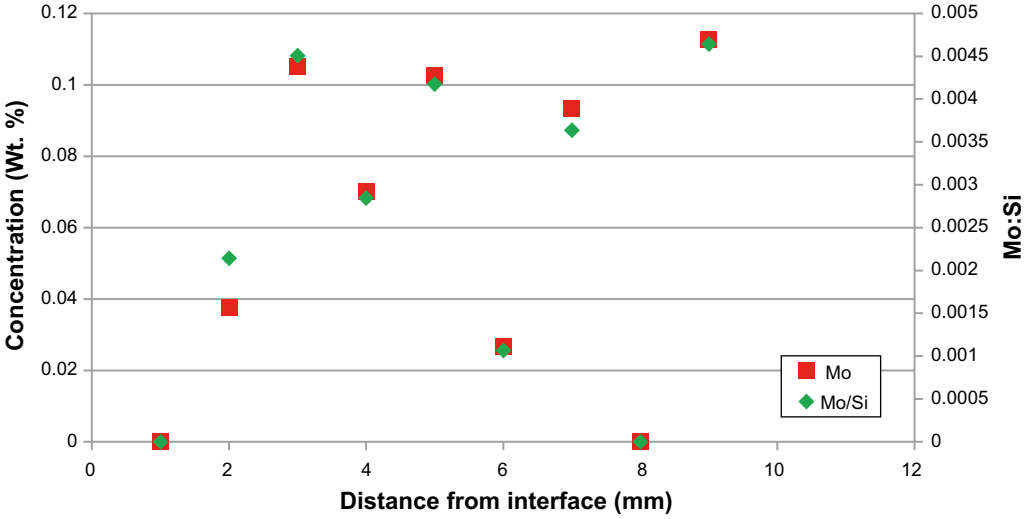

Figure 5-22. *Concentration profile of molybdenum in Ibeco RWC bentonite, specimen FXM000715.*

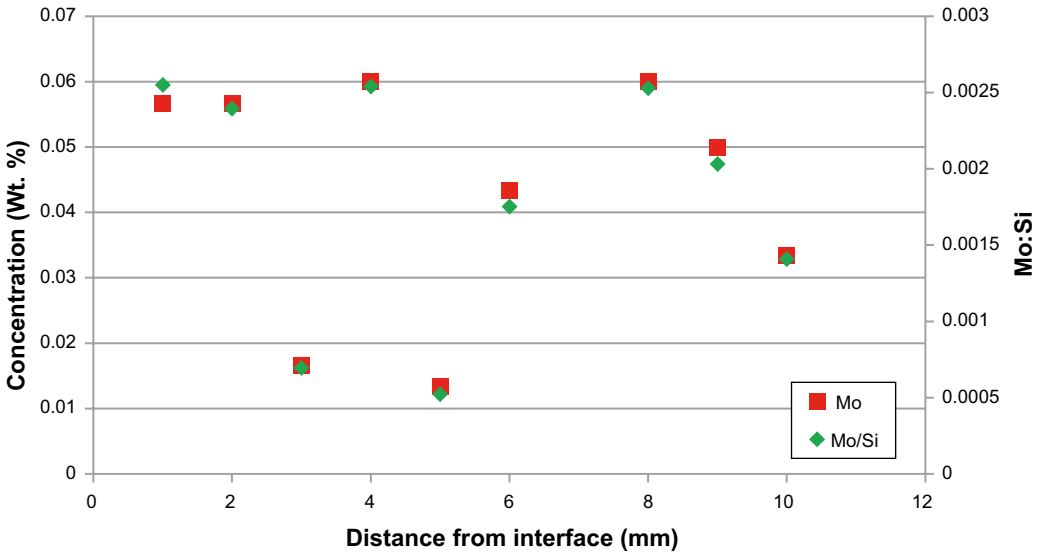

Figure 5-23. *Concentration profile of molybdenum in Ibeco RWC bentonite, specimen FXM000736.*

5.3.4 MX-80 bentonite

Caesium

Diffusion of Cs in MX-80 bentonite was studied using specimens FXM000763 and FXM000764. In both these specimens the small cylinders containing the CsCl powder were made of standard cement paste.

As for the other types of bentonite Figures 5-24 and 5-25 show a significant increase in the Cs concentration close to the cement/bentonite interface. The levels of Cs are well above the detection limit for the method and also much higher than the background level of Cs in MX-80 bentonite, Table 5-1. It can therefore be concluded that considerable amounts of Cs have been released from the cement specimen and also that diffusion of Cs in the bentonite has been significant.

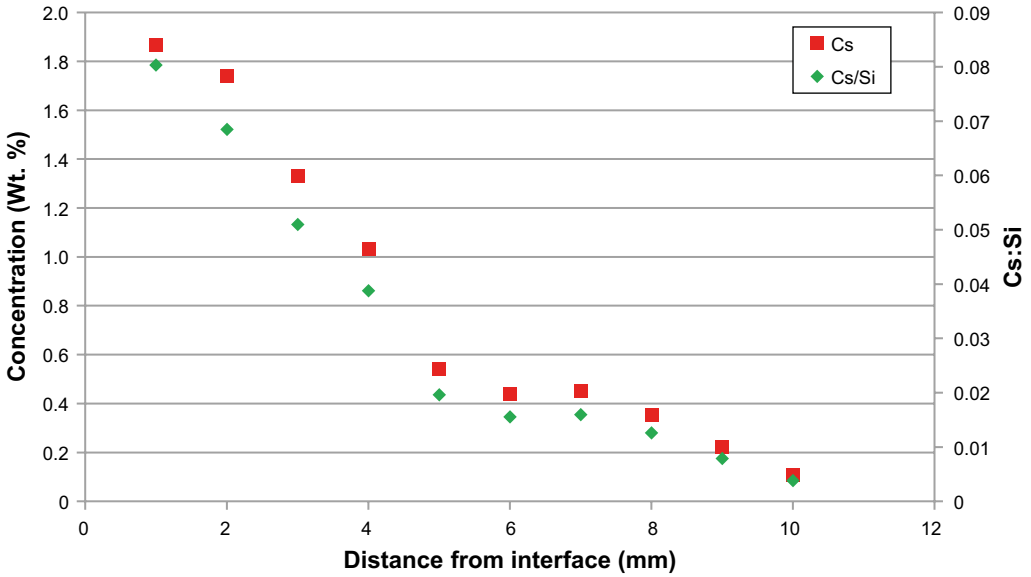

Figure 5-24. *Concentration profile of caesium in MX-80 bentonite, specimen FXM000764.*

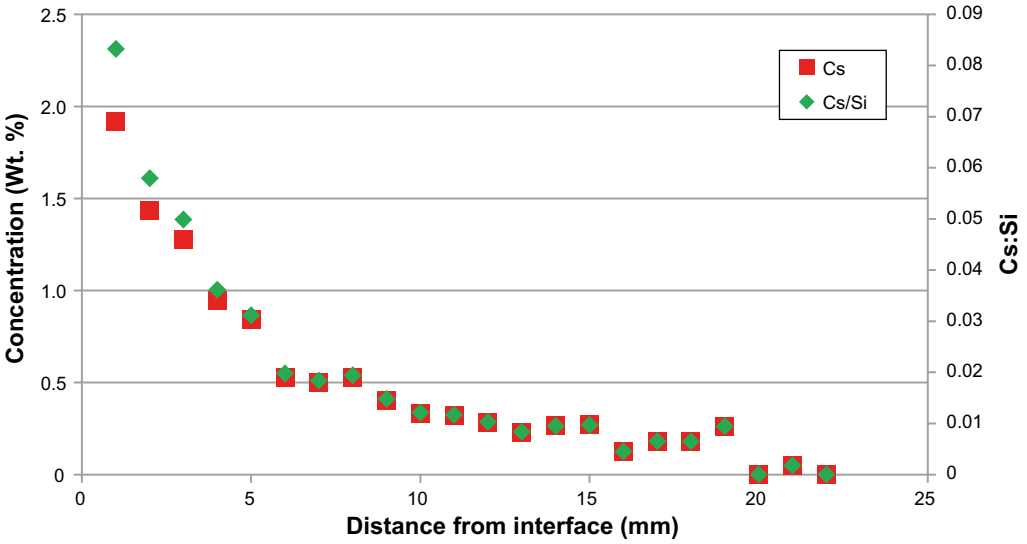

Figure 5-25. *Concentration profile of caesium in MX-80 bentonite, specimen FXM000763.*

Strontium

Diffusion of Sr in MX-80 bentonite was studied using specimen FXM000758. In this specimen the small cylinder containing the $SrCl_2$ powder was made of standard cement paste. Here, the analyses could not detect any Sr at all in the bentonite.

Europium

Diffusion of Eu in MX-80 bentonite was studied using specimens FXM000761 and FXM000762. In both specimens the small cylinders containing the $EuCl_3$ powder were made of standard cement paste.

The Eu concentrations found in the MX-80 bentonite, Figures 5-26 and 5-27, were below or very close to the detection limit for the method used (0.1%) and also in the same range as the background level of Eu in MX-80. Based on this it can be concluded that Eu release from the cement specimens has been minute even though it cannot be proven with certainty that no release has occurred.

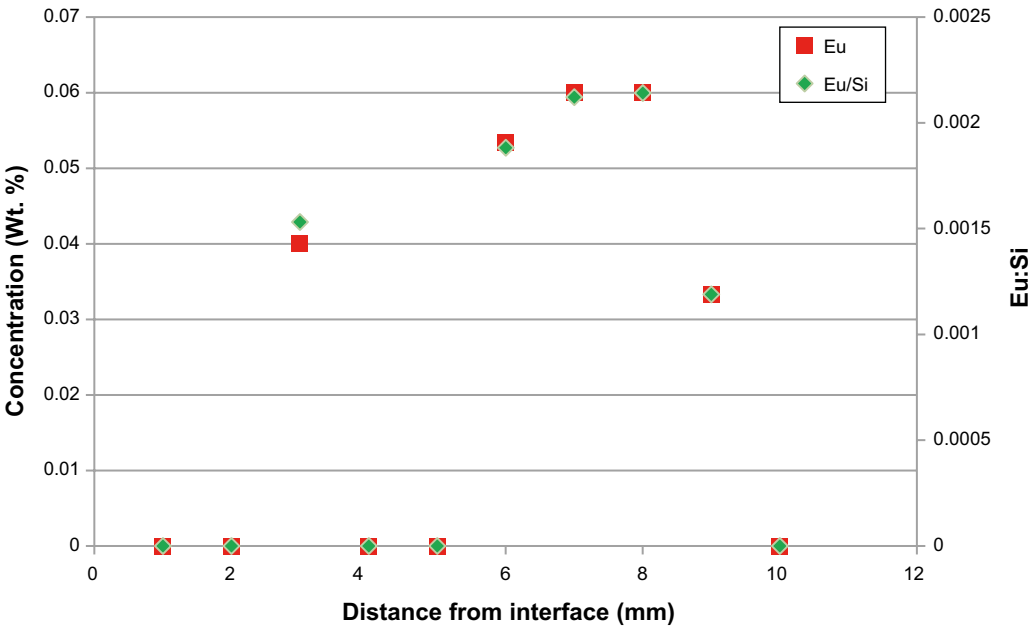

Figure 5-26. *Concentration profile of europium in MX-80 bentonite, Specimen FXM000761.*

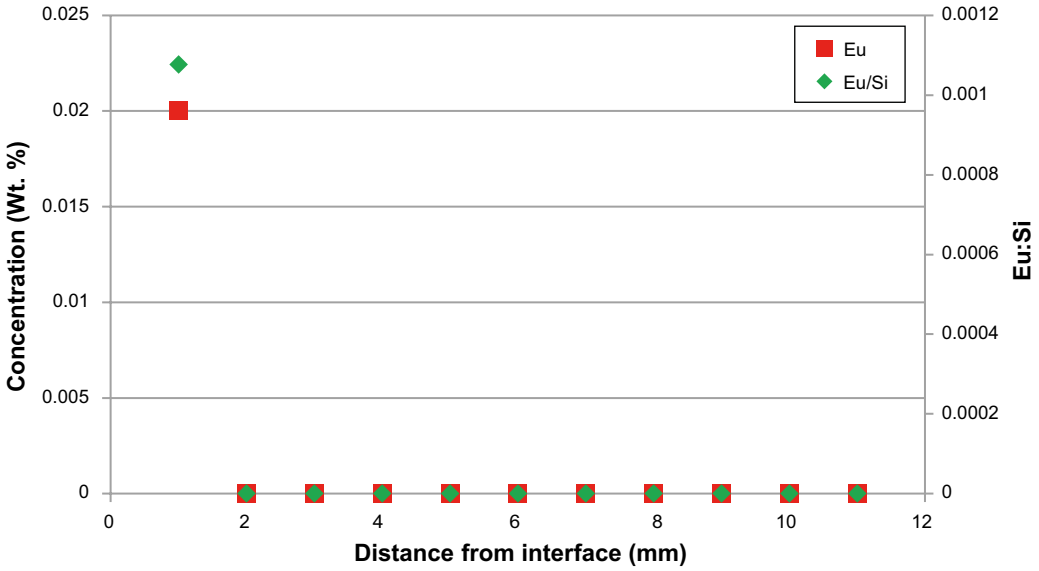

Figure 5-27. *Concentration profile of europium in MX-80 bentonite, Specimen FXM000762.*

Iron

Diffusion of Fe in MX-80 bentonite was studied using specimens FXM000745 and FXM000766. In FXM000745 the cement cylinder containing the Fe powder was made of standard cement paste whereas in FXM000766 it was made of low-pH cement paste.

The Fe concentrations found in the Febex bentonite were significant but with only small variations between the cement-bentonite interface and areas further into the bentonite, Figure 5-28 and 5-29. The levels found are also in close agreement with the background level of Fe in MX-80 bentonite, Table 5-1. Based on this it can be concluded that Fe release from the cement specimens has been low even though it cannot be proven with certainty that no release has occurred.

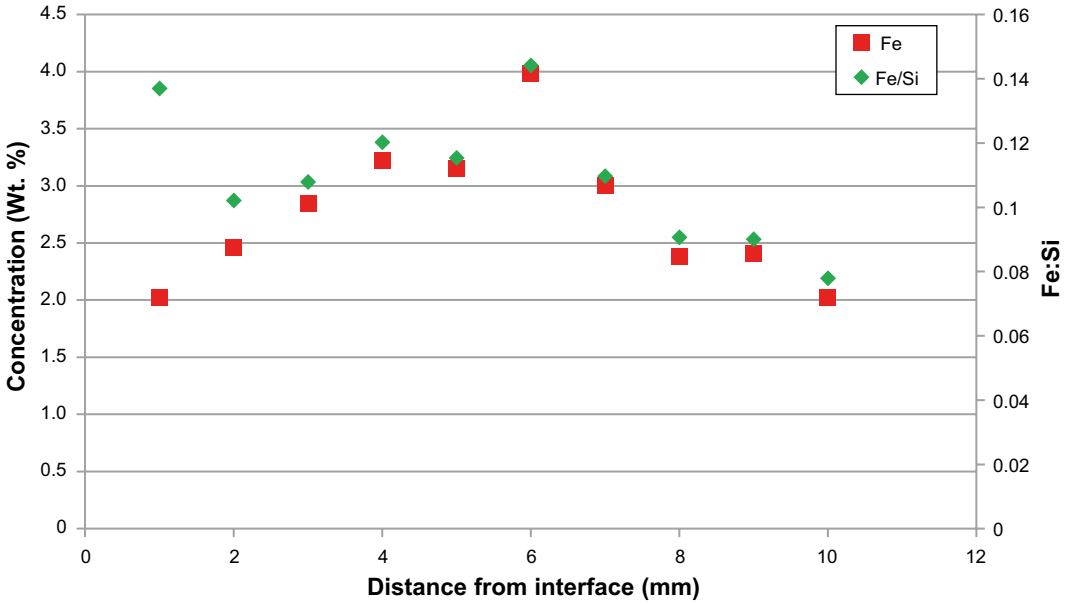

Figure 5-28. *Concentration profile of iron in MX-80 bentonite, Specimen FXM000745.*

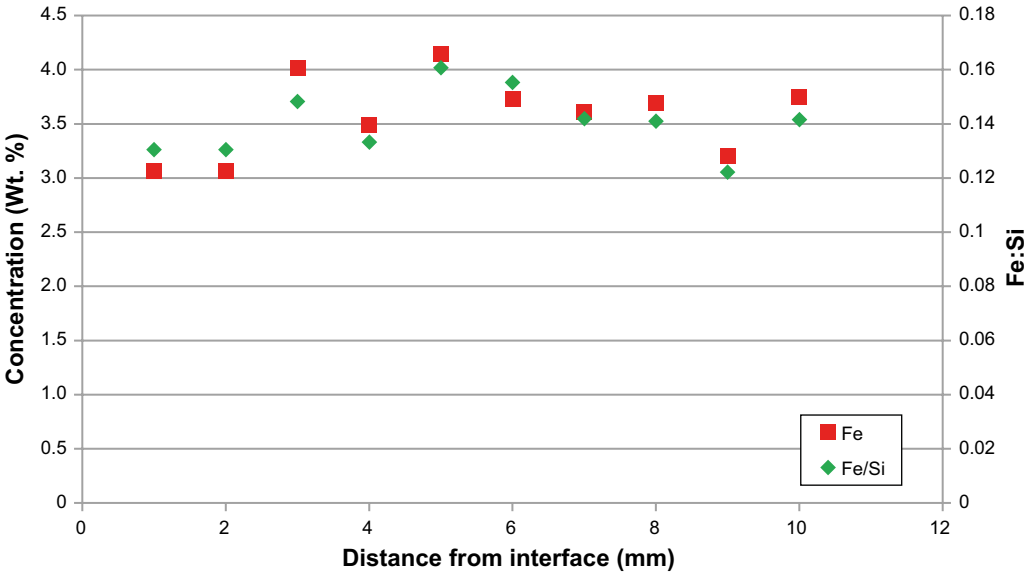

Figure 5-29. *Concentration profile of iron in MX-80 bentonite, specimen FXM000766.*

Nickel

Diffusion of Ni in MX-80 bentonite was not studied in this work.

Chromium

Diffusion of Cr in MX-80 bentonite was not studied in this work.

Molybdenum

Diffusion of Mo in MX-80 bentonite was studied using specimens FXM000747 and FXM000768. In FXM000747 the small cylinder containing the Mo powder was made of standard cement paste whereas in FXM000768 it was made of low-pH cement paste.

The Mo concentrations found in the MX-80 bentonite, Figures 5-30 and 5-31, were below or very close to the detection limit for the method used (0.1 %) and also in the same range as the background level of Mo in MX-80. Based on this it can be concluded that Mo release from the cement specimens has been minute even though it cannot be proven with certainty that no release has occurred.

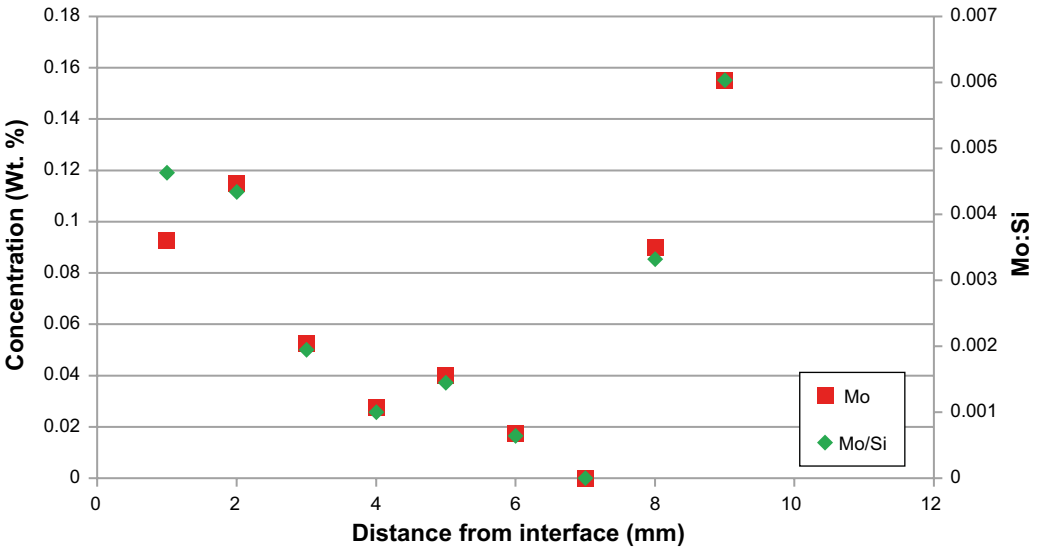

Figure 5-30. *Concentration profile of molybdenum in MX-80 bentonite, Specimen FXM000747.*

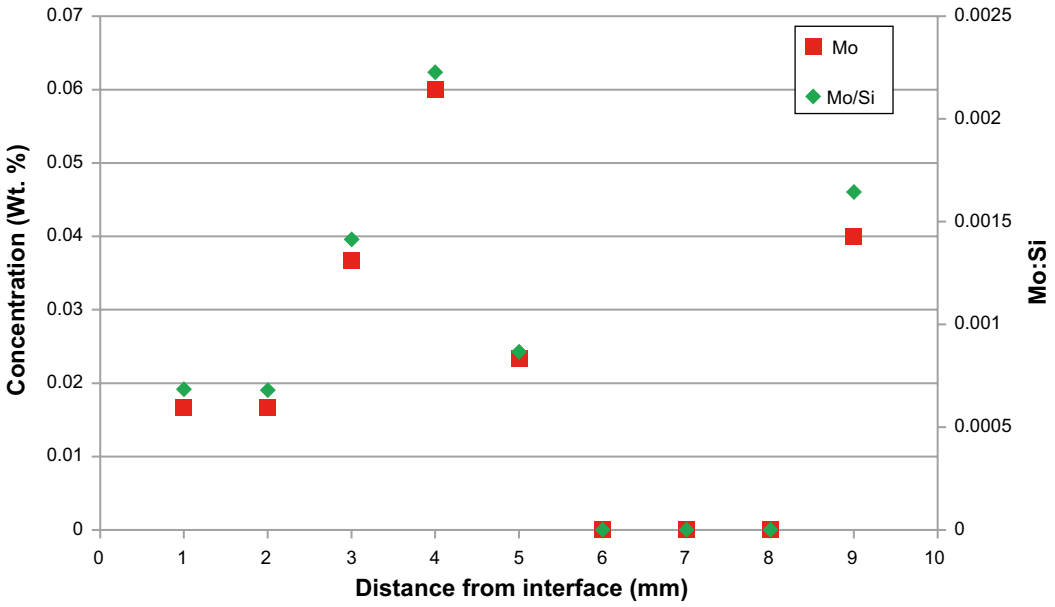

Figure 5-31. *Concentration profile of molybdenum in MX-80 bentonite Specimen FXM000768.*

5.4 Summary

In this chapter studies of out-diffusion of 7 different elements (Cs, Sr, Eu, Fe, Ni, Mo and Cr) from cement specimens made of standard and/or low-pH cement paste and in-diffusion of these elements into 4 different types of bentonite were presented. In these studies, extensive diffusion could only be detected for Cs for which a clear diffusion profile was found in all types of bentonite. For the other elements the levels found in the bentonite were either below the detection limit of the method or close to the background level of the studied bentonite.

6 Cement/ bentonite interface interactions

In this chapter the results from the analyses of interfacial reactions involving the parent elements of the cement specimens and the different types of bentonite are presented and discussed. As mentioned in Section 1.2, the purpose of this part of the experiments was to investigate the degree of cement/ bentonite interactions with main focus on inter diffusion of the parent elements between these two material types. A further objective was to study differences in diffusion profiles involving interactions between bentonite and standard cement paste and low-pH cement paste respectively.

The data presented in the figures in this chapter are average values from the bentonite blocks which have been in contact with standard cement or low-pH cement regardless of type of trace element in the small cement specimens. Typically the presented data are average values from 2-6 different specimens. This means that the statistical basis is rather limited and that one outlying value can have a significant impact on the presented results.

6.1 Asha bentonite

6.1.1 Interactions with cement specimens made of standard cement

Elemental composition of the bentonite close to the interface

Concentration profiles for C, Al, Ca, Mg and Si from the cement/bentonite interface to 8 mm into the bentonite are shown in Figure 6-1. From this figure, the concentration of Ca, C and Mg is higher close to the interface than further into the bentonite whereas the opposite applies for Al and Si. The elevated levels close to the interface is verified in Figure 6-5 where the Ca:Si and Mg:Si ratios for Asha bentonite in contact with standard and low-pH cement paste specimens are shown.

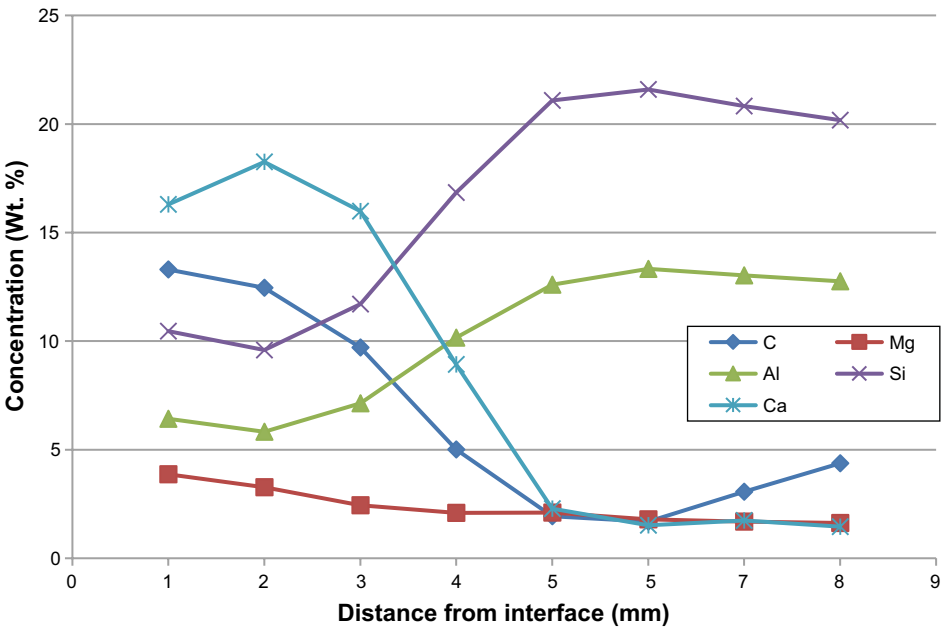

Figure 6-1. *Concentration profiles for C, Al, Ca, Mg and Si in the first 8 mm from the cement/bentonite interface for standard cement in contact with Asha bentonite.*

Visual appearance of the bentonite at the interface

In Figure 6-2 the contact zones of two samples of Asha bentonite that have been in contact with specimens made of standard cement paste are shown. Both images show a thin zone with different colour and structure than the bulk of the material. The visual appearance of this zone may in part be an effect of that the small slit that was formed between the cement specimen and the bentonite was filled with compacted bentonite powder during specimen preparation, probably giving a somewhat lower original density than the bulk bentonite. This does not, however, explain the colour difference in this zone.

Visual appearance of the cement specimen

Figure 6-3 shows the surface of a cement specimen that has been in contact with Asha bentonite. The surface presents a pattern with a similar appearance as the surface of the bentonite at the interface zone but no major transformations seem to have taken place.

Figure 6-2. *Images of the bentonite in the interface zone between Asha bentonite and specimens made of standard cement paste. Specimen FXM000778 (left, Fe) and FXM000780 (right, Mo).*

Figure 6-3. *Image of a cylinder made of standard cement paste that has been in contact with Asha bentonite. Specimen FXM000778 (Fe).*

6.1.2 Interactions with cement specimens made of Low-pH cement

Elemental composition of the bentonite close to the interface

Concentration profiles for C, Al, Ca, Mg and Si from the cement/bentonite interface to 11 mm into the bentonite are shown in Figure 6-4. The concentration profiles show only a slight increase in the relative levels of Ca and C close to the interface whereas Al and Si show somewhat reduced relative levels close to the interface than further into the bentonite.

The slightly elevated levels close to the interface are also indicated in Figure 6-5 where the Ca:Si and Mg:Si ratios for Asha bentonite in contact with standard and low-pH cement paste specimens are shown. Here the large difference in the Ca:Si ratio for the interfacial zone in Asha bentonite in contact with standard and low-pH cement is clearly noticeable.

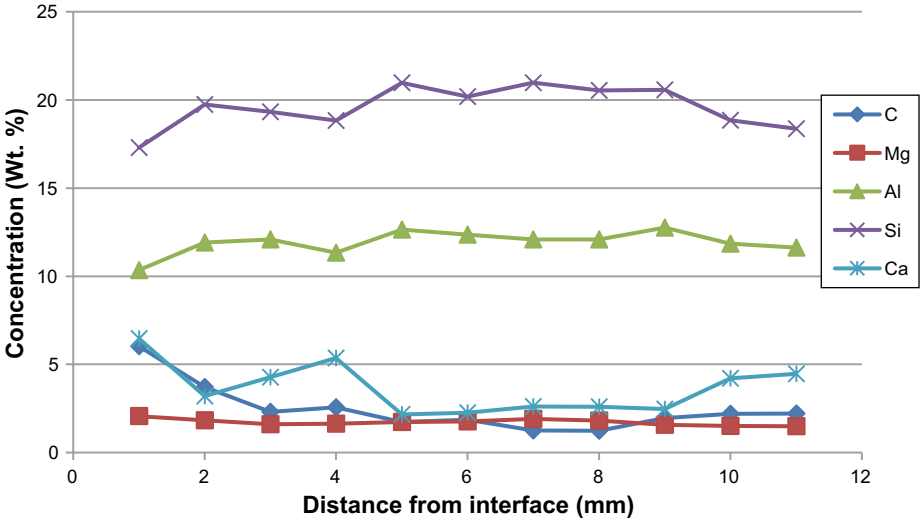

Figure 6-4. *Concentration profiles for Ca, Mg, Al, Si and C in the first 11 mm from the cement/bentonite interface for low-pH cement in contact with Asha bentonite.*

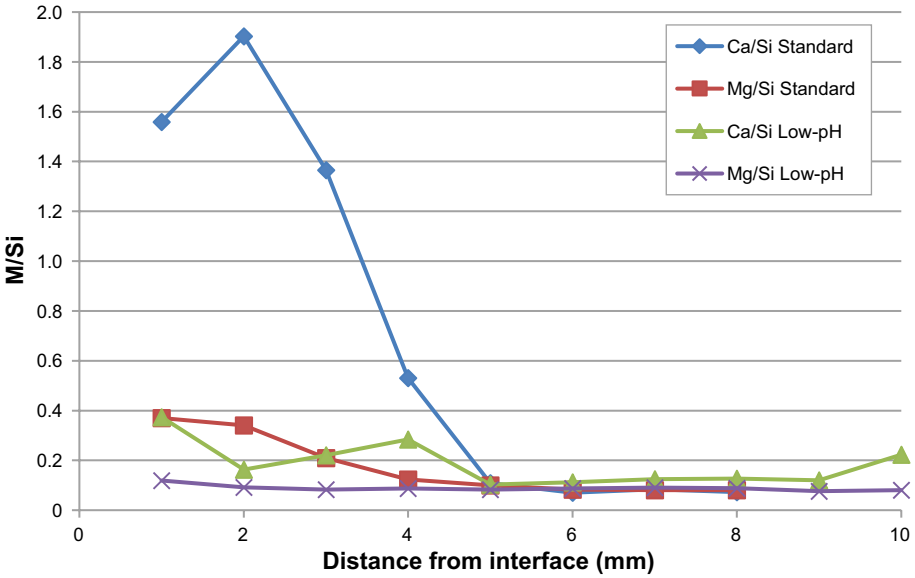

Figure 6-5. *Ca:Si and Mg:Si ratios in the first 10 mm from the cement/bentonite interface for standard cement and low-pH cement in contact with Asha bentonite.*

Visual appearance of the bentonite at the interface

From Figure 6-6 no clear indications of any transformations of the Asha bentonite that has been in contact with low-pH cement paste can be found.

Visual appearance of the cement specimen

Figure 6-7 shows the surfaces of cement specimens that have been in contact with Asha bentonite. The surface of the left specimen presents a pattern with a similar appearance as that of the specimen shown in Figure 6-3 whereas the right image shows a completely different appearance. This is, however, not reflected in the appearance of the bentonite surface that has been in contact with this specimen, Figure 6-6, right image.

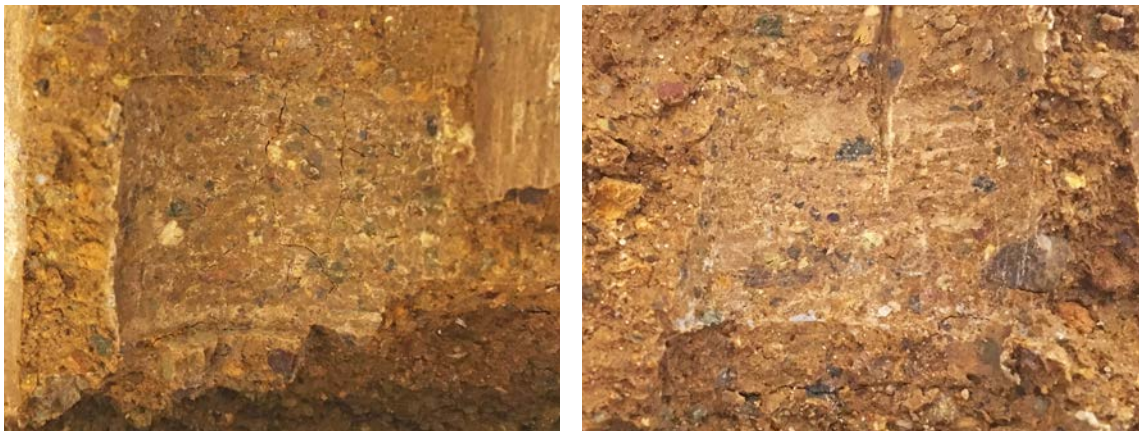

Figure 6-6. *Images of the bentonite (Asha) at the position where specimens of low-pH cement paste has been placed. Specimen FXM000798 (left, Fe) and FXM000799 (right, Mo).*

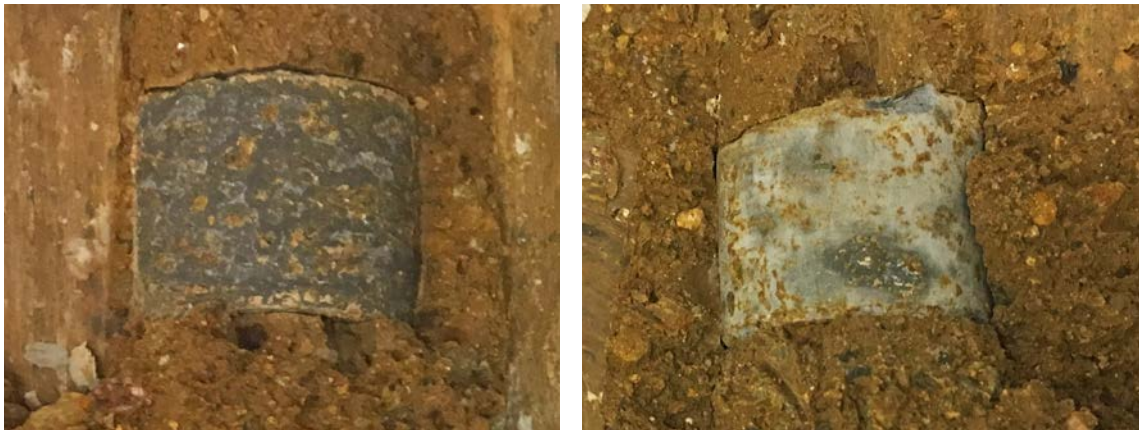

Figure 6-7. *Images of cylinders made of low-pH cement paste that has been in contact with Asha bentonite. Specimen FXM000798 (left, Fe) and FXM000799 (right, Mo).*

6.2 Febex bentonite

6.2.1 Interactions with cement specimens made of standard cement

Elemental composition of the bentonite close to the interface

Concentration profiles for C, Al, Ca, Mg and Si from the cement/bentonite interface to 10 mm into the bentonite are shown in Figure 6-8. From this figure, the concentration of Ca, C and Mg is higher close to the interface than further into the bentonite whereas the opposite applies for Al and Si. The elevated levels close to the interface is verified in Figure 6-12 where the Ca:Si and Mg:Si ratios for Febex bentonite in contact with standard and low-pH cement paste specimens are shown.

Visual appearance of the bentonite at the interface

In Figure 6-9 the contact zone of a sample of Febex bentonite that have been in contact with a specimen made of standard cement paste is shown. The image shows a thin zone which partly has a different colour and structure than the bulk of the material. The upper part of the interface zone also presents a layered appearance with a white crust closest to the cement specimen and a darker zone further into the transition zone. A dark piece of the cement specimen is also seen here.

Visual appearance of the cement specimen

Figure 6-10 shows the surface of the cement specimen that has been in contact with Febex bentonite. The surface presents a pattern with a similar appearance as the surface of the bentonite that has been in contact with the cement specimen but no major transformations seem to have occured.

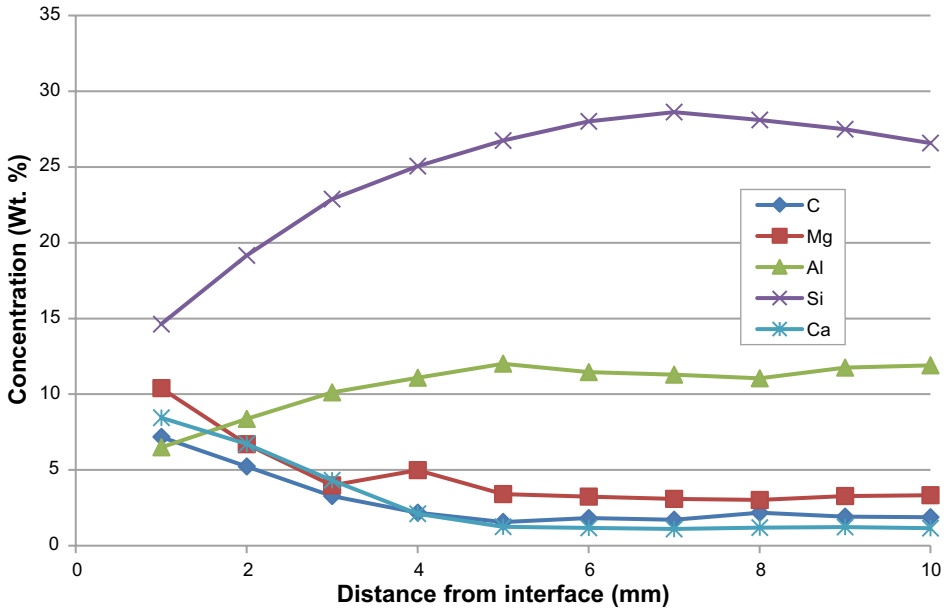

Figure 6-8. *Concentration profiles for Ca, Mg, Al, Si and C in the first 10 mm from the cement/bentonite interface for standard cement in contact with Febex bentonite.*

Figure 6-9. *Image of the bentonite (Febex) at the position where a specimen of standard cement paste has been placed. Specimen FXM000697 ($SrCl_2$).*

Figure 6-10. *Image of a cylinder made of standard cement paste that has been in contact with Febex bentonite. Specimen FXM000697 ($SrCl_2$).*

6.2.2 Interactions with cement specimens made of Low-pH cement

Elemental composition of the bentonite close to the interface

Concentration profiles for C, Al, Ca, Mg and Si from the cement/bentonite interface to 10 mm into the bentonite are shown in Figure 6-11. The concentration profiles show only a slight increase in the relative levels of Ca, Mg and C close to the interface whereas Al and Si show somewhat reduced relative levels close to the interface than further into the bentonite.

The slightly elevated levels close to the interface are also indicated in Figure 6-12 where the Ca:Si and Mg:Si ratios for Febex bentonite in contact with standard and low-pH cement paste specimens are shown. Here the large difference in the Ca:Si ratio for the interfacial zone in Febex bentonite in contact with standard and low-pH cement is clearly noticeable.

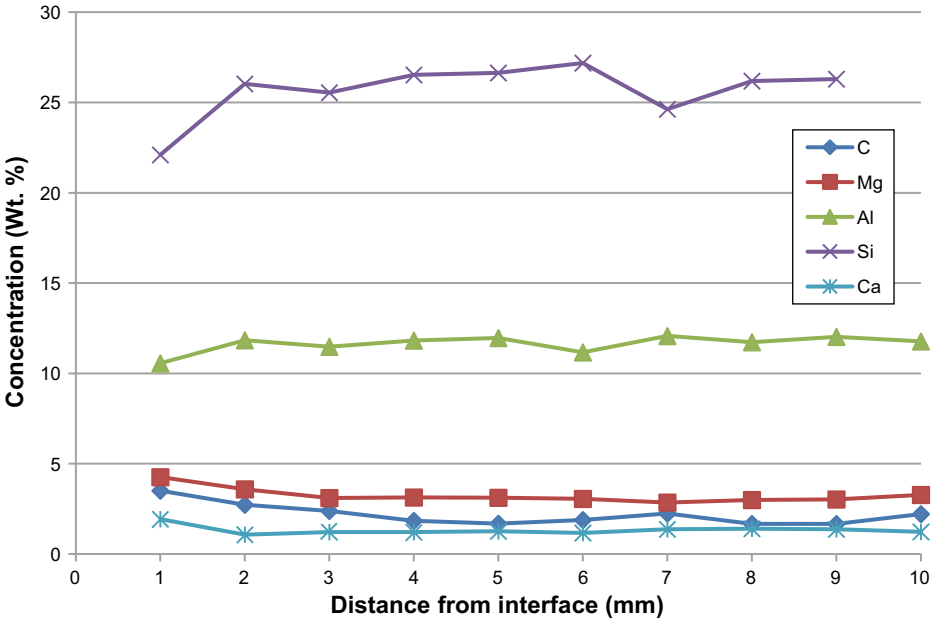

Figure 6-11. *Concentration profile for Ca, Mg, Al, Si and C in the first 10 mm from the cement/bentonite interface for low-pH cement in contact with Febex bentonite.*

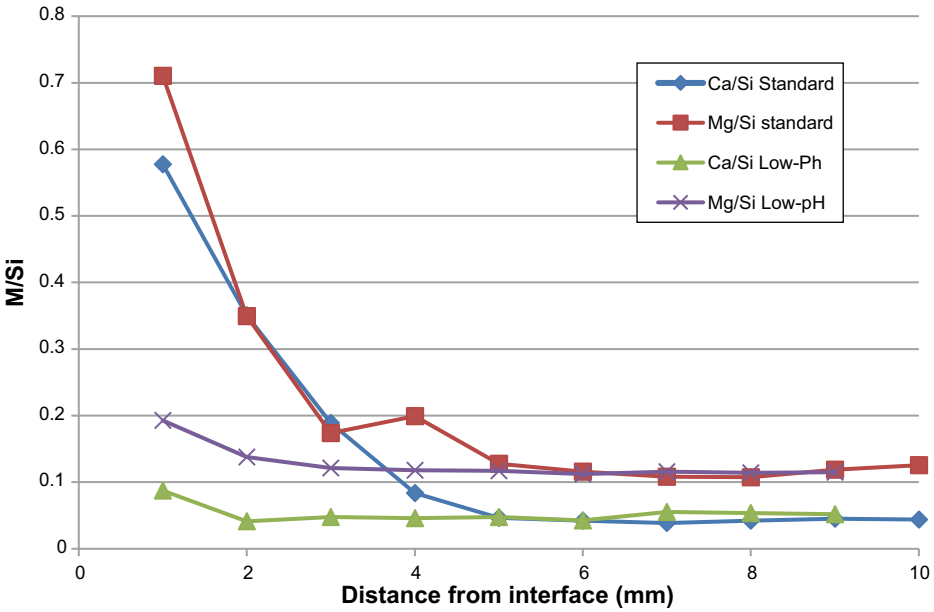

Figure 6-12. *Ca:Si and Mg:Si ratios in the first 10 mm from the cement/bentonite interface for standard cement and low-pH cement in contact with Febex bentonite.*

Visual appearance of the bentonite at the interface

From Figure 6-13 a slight change in colour of the Febex bentonite that has been in contact with low-pH cement paste compared with the bulk bentonite reflected as a somewhat whiter crust than the bulk of the material can be noticed. The structural difference of the bentonite at the interfacial zone shown in Figure 6-9 is however not found in this specimen.

Visual appearance of the cement specimen

Figure 6-14 shows the surfaces of a low-pH cement specimen containing molybdenum that has been in contact with Febex bentonite. The surface of the specimen has a whitish/light greyish appearance resembling that of the specimen shown in the right image in Figure 6-7.

Figure 6-13. *Image of the bentonite (Febex) at the position where a specimen of low-pH cement paste has been placed. Specimen FXM000708 (Mo).*

Figure 6-14. *Image of a cylinder made of low-pH cement paste that has been in contact with Febex bentonite. Specimen FXM000708 (Mo).*

6.3 Ibeco RWC bentonite

6.3.1 Interactions with cement specimens made of standard cement

Elemental composition of the bentonite close to the interface

Concentration profiles for C, Al, Ca, Mg and Si from the cement/bentonite interface to 10 mm into the bentonite are shown in Figure 6-15. From this figure, the concentrations of Ca, C and Mg are higher close to the interface than further into the bentonite whereas the opposite applies for Al and Si.

The elevated levels close to the interface is verified in Figure 6-19 where the Ca:Si and Mg:Si ratios for Ibeco RWC bentonite in contact with standard and low-pH cement paste specimens are shown.

Visual appearance of the bentonite at the interface

In Figure 6-16 the contact zones of samples of Ibeco RWC bentonite that have been in contact with specimens made of standard cement paste are shown. The images show a thin zone which partly has a different colour and structure than the bulk of the material. Parts of the interface zone also present a layered appearance with a white crust closest to the cement specimen and a darker zone further into the transition zone. Compare also with Figure 6-9 which shows a very similar appearance for the Febex bentonite.

Visual appearance of the cement specimen

Figure 6-17 shows the surface of a cement specimen that has been in contact with Ibeco RWC bentonite. The surface does not present any clear transformations but some small white areas are found close to the edges of the specimen.

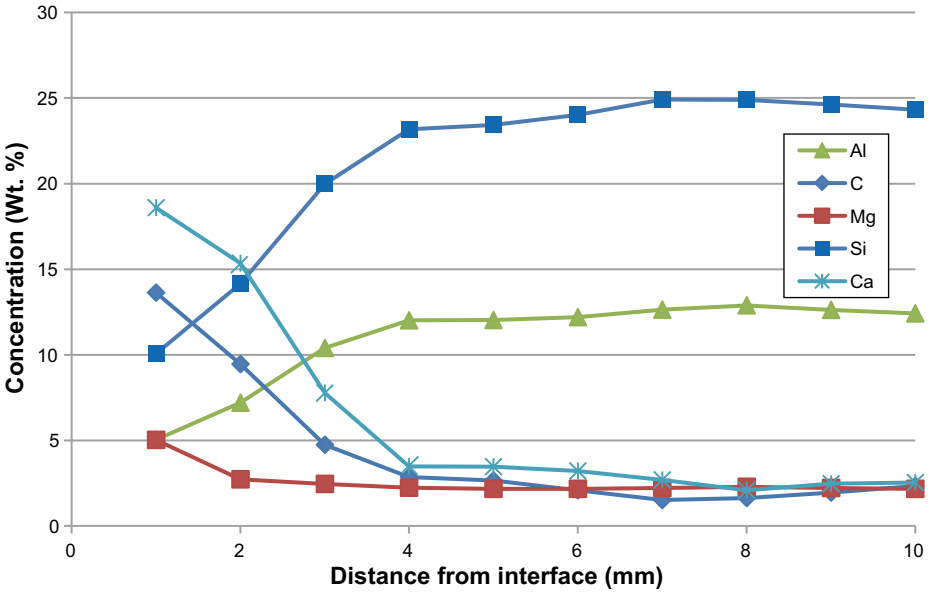

Figure 6-15. *Concentration profiles for Ca, Mg, Al, Si and C in the first 10 mm from the cement/bentonite interface for standard cement in contact with Ibeco RWC bentonite.*

Figure 6-16. *Images of Ibeco RWC bentonite at the position where specimens of standard cement paste have been placed. Specimen FXM000714 (top left, Fe), FXM000725 (top right $SrCl_2$) and FXM000732 (lower left, CsCl).*

Figure 6-17. *Image of a cylinder made of standard cement paste that has been in contact with Ibeco RWC bentonite. Specimen FXM000714 (Fe).*

6.3.2 Interactions with cement specimens made of Low-pH cement

Elemental composition of the bentonite close to the interface

Concentration profiles for C, Al, Ca, Mg and Si from the interface between the cement paste specimens and to 10 mm into the bentonite are shown in Figure 6-18. The concentration profiles show a distinct increase in the relative levels of Ca and C close to the interface whereas Al and Si show somewhat reduced relative levels in this part of the specimen than further into the bentonite. However, it should be noticed that the values presented in Figure 6-18 and are average values from only 2 specimens. For Ca at a distance of 1 mm from the interface, the respective values forming this average are 2.58 % and 26.68 % respectively. This means that the uncertainties in this data point are very large and the correctness of the average value can be questioned. These uncertainties should also be recalled when studying the Ca:Si and Mg:Si ratios for Ibeco RWC bentonite in contact with standard and low-pH cement paste specimens shown in Figure 6-19.

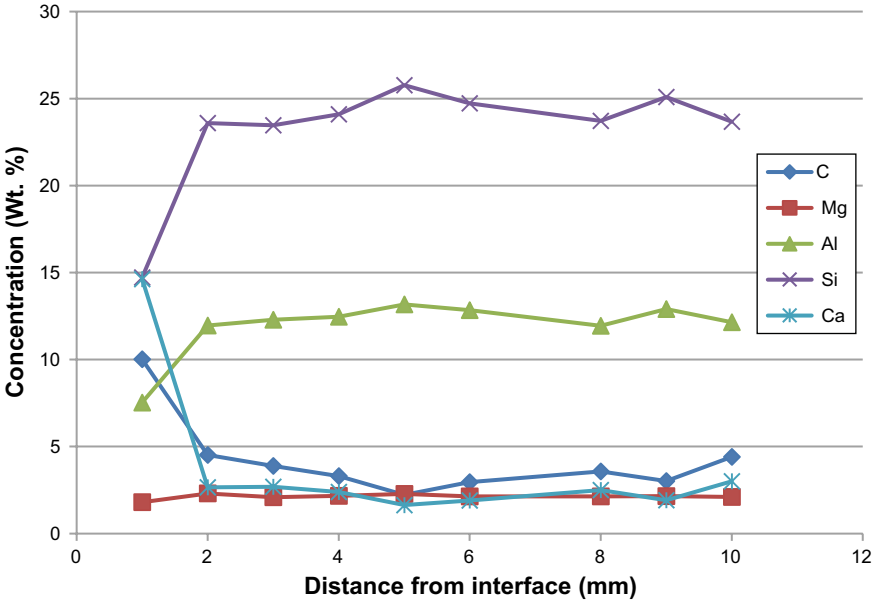

Figure 6-18. *Concentration profiles for Ca, Mg, Al, Si and C in the first 10 mm from the cement/bentonite interface for low-pH cement in contact with Ibeco RWC bentonite.*

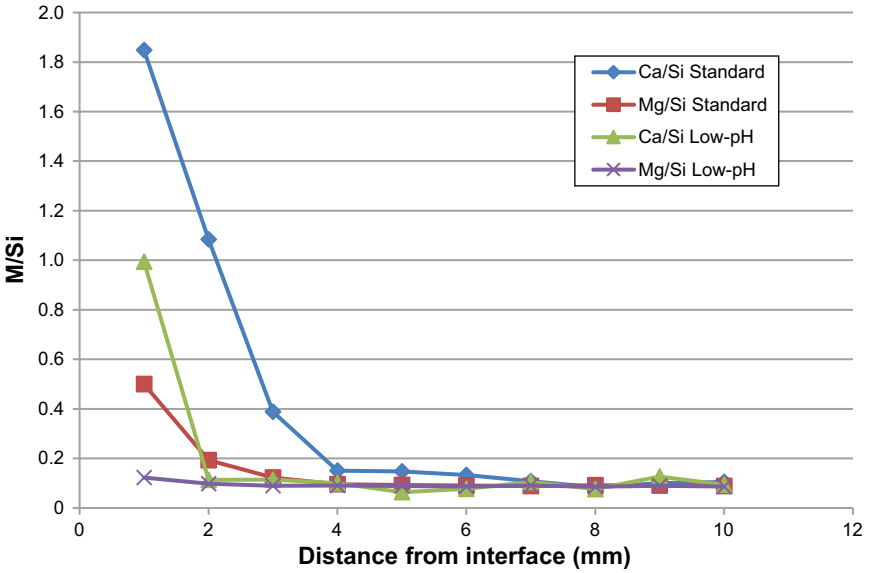

Figure 6-19. *Ca:Si and Mg:Si ratios in the first 10 mm from the cement/bentonite interface for standard cement and low-pH cement in contact with Ibeco RWC bentonite.*

Visual appearance of the bentonite at the interface

From Figure 6-20 only a slight change in structure of the Ibeco RWC bentonite that has been in contact with low-pH cement paste compared with the bulk bentonite can be noticed. The colour of the bentonite in the interface zone is also more or less the same as that of the bulk bentonite.

Visual appearance of the cement specimen

Figure 6-21 shows the surface of a cement specimen containing molybdenum that has been in contact with Ibeco RWC bentonite. The surface of the specimen has a whitish/light greyish appearance resembling that of the specimens shown in the right image in Figure 6-7 as well as in Figure 6-14, both of which also contains molybdenum. Also, as with the Asha bentonite shown in Figure 6-6 (right image) this is not obviously reflected in the appearance of the bentonite surface that has been in contact with this specimen, Figure 6-20.

Figure 6-20. *Image of the bentonite at the position where a specimen of low-pH cement paste has been placed. Specimen FXM000736 (Mo).*

Figure 6-21. *Image of a cylinder made of low-pH cement paste that has been in contact with Ibeco RWC bentonite. Specimen FXM000736 (Mo).*

6.4 MX-80 bentonite

6.4.1 Interactions with cement specimens made of standard cement

Elemental composition of the bentonite close to the interface

Concentration profiles for C, Al, Ca, Mg and Si from the cement/bentonite interface to 10 mm into the bentonite are shown in Figure 6-22. From this figure, the concentration of Ca, C and Mg is only slightly higher close to the interface than further into the bentonite whereas the opposite applies for Al and Si.

The elevated levels close to the interface are also shown in Figure 6-26 where the Ca:Si and Mg:Si ratios for MX-80 bentonite in contact with standard and low-pH cement paste specimens are shown.

Visual appearance of the bentonite at the interface

In Figure 6-23 the contact zones of samples of MX-80 bentonite that have been in contact with specimens made of standard cement paste are shown. The images clearly show that a bright zone with a larger thickness than observed for the other types of bentonite has developed at the interface in all specimens.

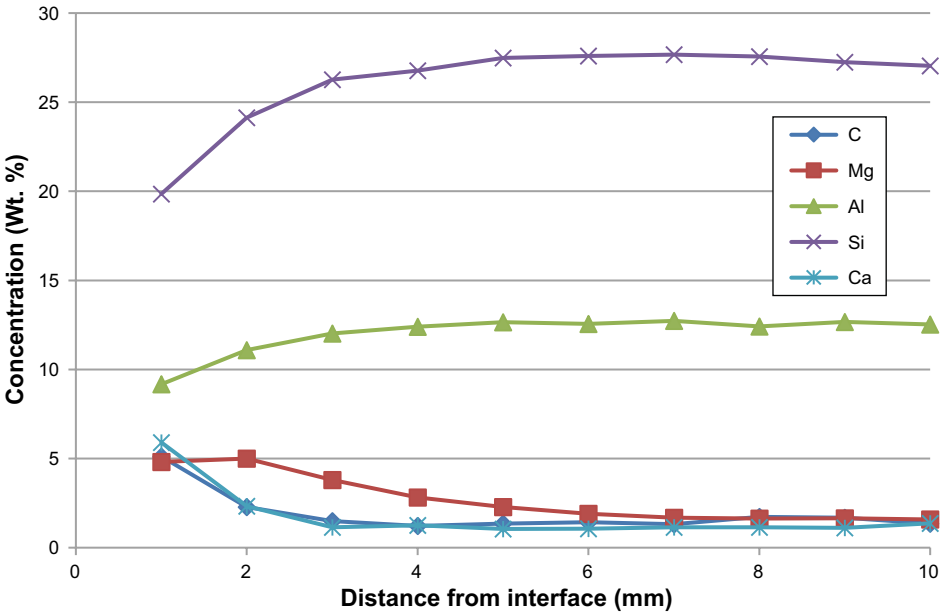

Figure 6-22. *Concentration profiles for Ca, Mg, Al, Si and C in the first 10 mm from the cement/bentonite interface for standard cement in contact with MX-80 bentonite.*

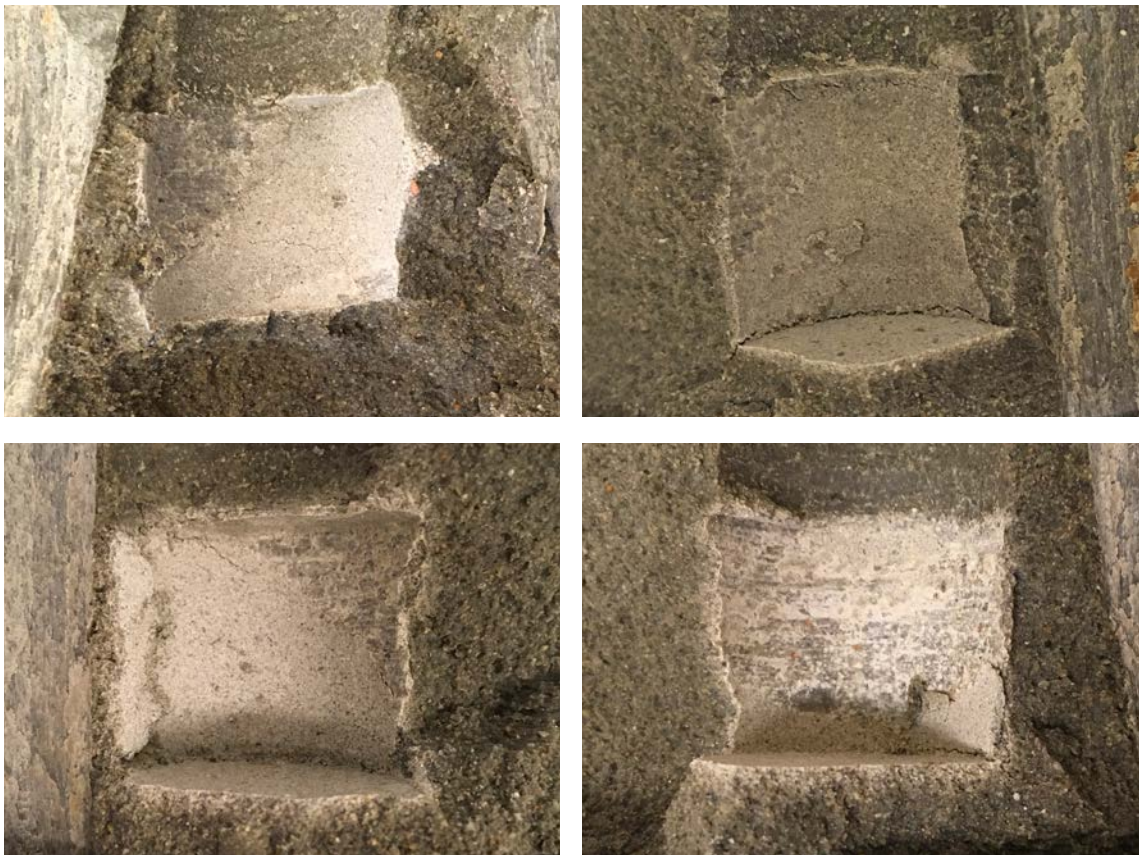

Figure 6-23. *Images of the bentonite at the position where specimens of standard cement paste have been placed. Specimen FXM000745 (top left, Fe), FXM000747 (top right, Mo), FXM000761 (lower left, $EuCl_3$) and FXM000762 (lower right, $EuCl_3$).*

Visual appearance of the cement specimen

Figure 6-24 shows the surfaces of cement specimens that have been in contact with MX-80 bentonite. The surfaces of both specimens are clearly brighter than most of the cement specimens investigated in this study.

Figure 6-24. *Images of cylinders made of standard cement paste that have been in contact with MX-80 bentonite. Specimen FXM000745 (left, Fe) and FXM000761 (right, $EuCl_3$).*

6.4.2 Interactions with cement specimens made of Low-pH cement

Elemental composition of the bentonite close to the interface

Concentration profiles for C, Al, Ca, Mg and Si from the cement/bentonite interface to 10 mm into the bentonite are shown in Figure 6-25. From this figure, only very small increases in the relative levels of Ca and Mg close to the interface can be observed whereas the variations in the relative concentrations of the other elements are within measurement uncertainties and natural variations within the specimens.

The slightly elevated levels close to the interface are also shown in Figure 6-26 where the Ca:Si and Mg:Si ratios for MX-80 bentonite in contact with standard and low-pH cement paste specimens are shown. Here the large difference in the Ca:Si ratio for the interfacial zone in MX-80 bentonite in contact with standard and low-pH cement respectively is clearly noticeable. Also, the Ca:Si and Mg:Si ratios are much lower for MX-80 bentonite than for the other types of bentonite.

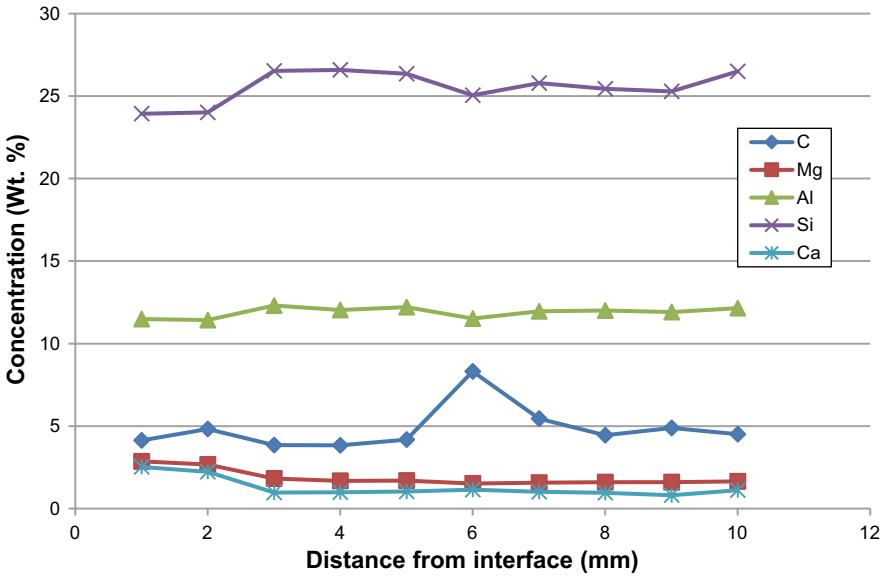

Figure 6-25. *Concentration profile for Ca, Mg, Al, Si and C in the first 10 mm from the cement/bentonite interface for low-pH cement in contact with MX-80 bentonite.*

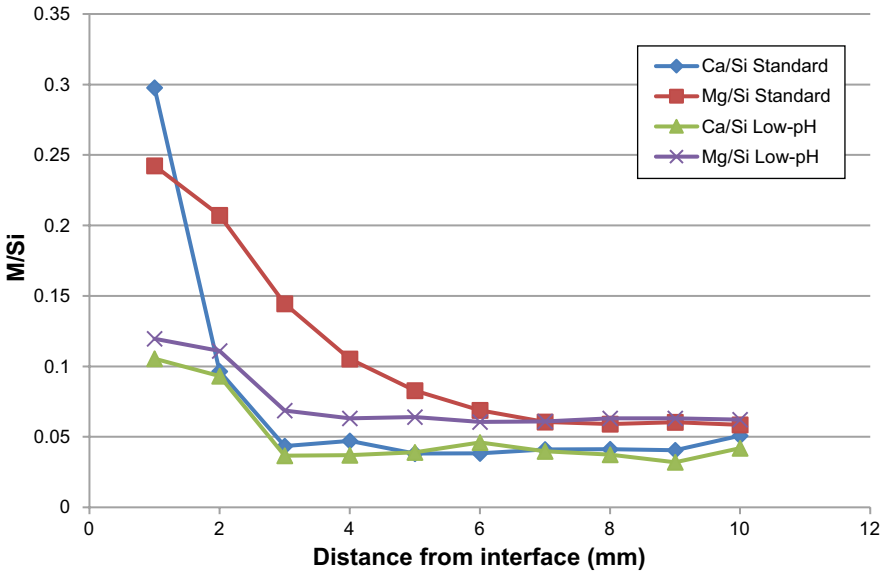

Figure 6-26. *Ca:Si and Mg:Si ratios in the first 10 mm from the cement/bentonite interface for standard cement and low-pH cement in contact with MX-80 bentonite.*

Visual appearance of the bentonite at the interface

In Figure 6-27 the contact zones of samples of MX-80 bentonite that have been in contact with specimens made of low-pH cement paste are shown. The images show that a thin zone which is much brighter than the bulk bentonite has developed at the interface shown in the left image whereas the colour of the interfacial bentonite shown in the right image more resembles that of the bulk bentonite.

Visual appearance of the cement specimen

Figure 6-28 shows the surfaces of cement specimens that have been in contact with MX-80 bentonite. The surface of the left specimen does not show any major evidences of transformation with only a few white spots in an otherwise grey matrix. For the right hand specimen on the other side, the surface of the specimen has a whitish/light greyish appearance resembling that of the specimen shown in the right image in Figure 6-7. Also, as with the Asha bentonite shown in Figure 6-6 this is not obviously reflected in the appearance of the bentonite surface that has been in contact with this specimen, Figure 6-27, right image. Interestingly all cement specimens that have shown a white/light grey surface have contained molybdenum, suggesting that this metal one way or another is responsible for this change in colour.

Figure 6-27. *Images of the bentonite at the position where specimens of low-pH cement paste have been placed. Specimen FXM000766 (left, Fe) and FXM000768 (right, Mo).*

Figure 6-28. *Images of cylinders made of low-pH cement paste that have been in contact with MX-80 bentonite. Specimen FXM000766 (left, Fe) and FXM000768 (right, Mo).*

6.5 Elemental composition of the cement paste specimens

Figure 6-29 shows the Ca:Si ratio in the specimens made of standard cement paste at different distances from the cement-bentonite interface for standard cement paste embedded in all types of bentonite. As shown in this figure, a somewhat reduced Ca:Si ratio is observed closer to the interface than further into the cement specimen. However, the trend is not clear for all types of bentonite due to poor statistics. Unfortunately, no data were available for specimens made of low-pH cement paste.

6.6 Summary

In this chapter cement/bentonite interface reactions involving only the parent elements of the materials were investigated. The results show that Ca and Mg diffusion has been more pronounced for bentonite in contact with specimens made of standard cement paste than for those in contact with low-pH specimens. The studies also show increased levels of C in the bentonite close to the interface.

Studies of the visual appearance of the bentonite at the cement/bentonite interface revealed the presence of a whitish crust just at the contact zone for many of the specimens. Further, also a structurally different zone of bentonite with a maximum thickness of about 2 mm was observed for a number of specimens. When these observations are evaluated together with the results from the EDS analyses it is considered rather likely that the whitish crust found at the bentonite part of the interface consists of $CaCO_3$ and $MgCO_3$.

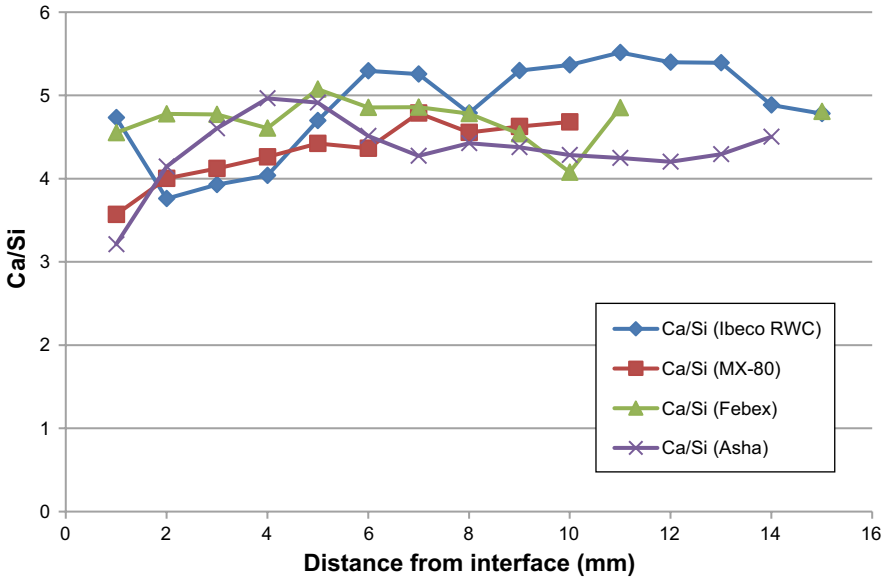

Figure 6-29. *Ca:Si-ratios for cement specimens made of standard cement that have been in contact with four different types of bentonite. Values are average values from all specimens regardless of which type of trace element they contained.*

7 Summary and conclusions

7.1 Summary

7.1.1 Retrieval, sectioning and segmentation

The most important experience from the retrieval of the package was that the original plan with direct retrieval without preceding over-coring did not work out at all. The main reason for this was that it was not possible to remove enough sand in the slit between the package and the wall of the installation hole. This, in turn, was caused by the swelling of the bentonite which both had compacted the sand but also caused an expansion of the cage in which the bentonite blocks were confined, thus closing the slit completely in some areas. Instead, conventional over-coring of the entire package was used. The method worked well even though some problems with fracturing of the released rock had to be handled.

Upon exposure of the package it was realised that the bolts holding the lid had been sheared of by the large swelling pressure of the bentonite and that the top 3 blocks had swelled more or less freely. During swelling, also the small cement specimens embedded in the bentonite blocks had moved up to 100 mm from their original positions. For that reason, these specimens were discarded.

Disassembling of the package, sectioning of the individual blocks, packaging in aluminium bags and labelling were performed according to standard procedures.

7.1.2 Diffusion of trace elements

In Chapter 5 studies of out-diffusion of 7 different elements (Cs, Sr, Eu, Fe, Ni, Mo and Cr) from cement specimens made of standard and/or low-pH cement paste and in-diffusion of these elements into 4 different types of bentonite were presented. In these studies, extensive diffusion could only be detected for Cs for which a clear diffusion profile was found in all types of bentonite. For the other elements the levels found in the bentonite were either below the detection limit of the method or close to the background level of the studied bentonite.

7.1.3 Cement/bentonite interface reactions

In Chapter 6 cement/bentonite interface reactions were investigated. The results from EDS analyses summarised in Figure 7-1 and 7-2 show that Ca and Mg diffusion in bentonite has been more pronounced for bentonite in contact with specimens made of standard cement paste than for low-pH specimens. Here, please recall the uncertainties regarding interactions between low-pH cement and Ibeco RWC as discussed in Section 6.3.2. Ca and Mg diffusion was also reflected in the elemental composition of the cement specimens which presented reduced levels of these elements close to the cement/bentonite interface.

Studies of the visual appearance of the bentonite at the cement/bentonite interface revealed the presence of a whitish crust just at the contact zone for many of the specimens. Further, also a structurally different zone of bentonite with a maximum thickness of about 2 mm was observed for a number of specimens. These effects were more pronounced for MX-80 type bentonite than for any of the other types of bentonite. However, as shown in Figure 7-1 and 7-2, this was not reflected in the elemental composition of the bentonite in this zone. When these observations are evaluated together with the results from the EDS analyses it is considered rather likely that the whitish crust found at the bentonite part of the interface consists of $CaCO_3$ and $MgCO_3$.

Finally, the visual appearance of the cement specimens was not clearly affected by the type of bentonite with which the specimens had been in contact. Instead, the most pronounced effect was that specimens containing molybdenum were much brighter than cement specimens containing any of the other elements.

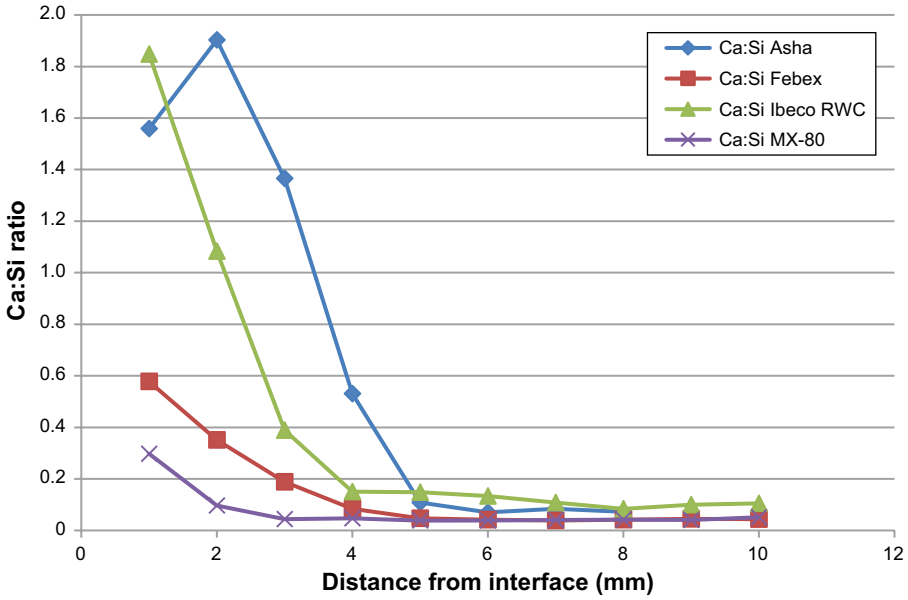

Figure 7-1. *Ca:Si ratio in the four different types of bentonite used in this study from the cement-bentonite interface and 10 mm into the bentonite. Here standard cement paste was used.*

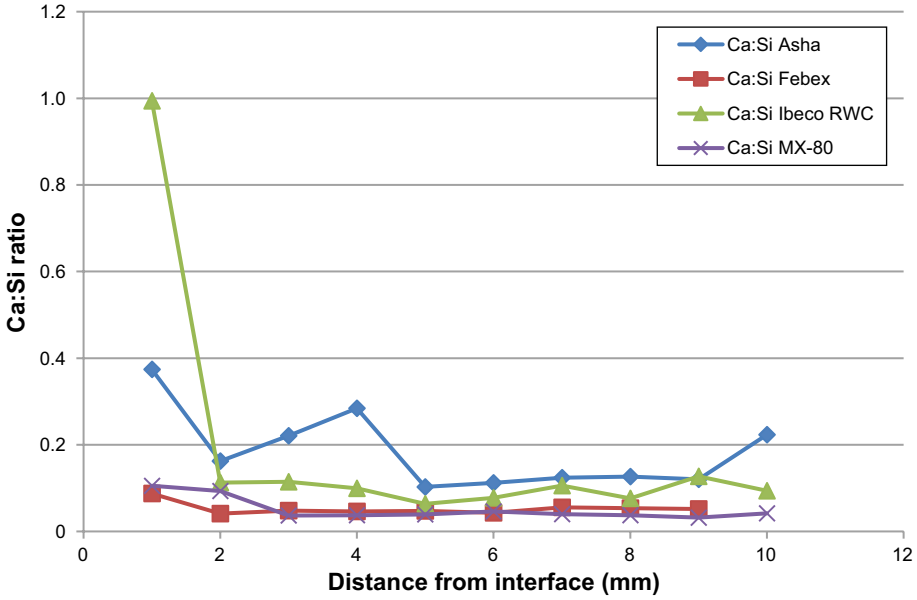

Figure 7-2. *Ca:Si ratio in the four different types of bentonite used in this study from the cement-bentonite interface and 10 mm into the bentonite. Here low-pH cement paste was used.*

7.2 Conclusions

In this report, experiences from retrieval of Concrete and Clay experiment # 20 and results from the analyses of diffusion of elements in the bentonite as well as cement/bentonite interactions have been reported. The following main conclusions can be drawn from this work:

- Retrieval of the remaining packages in this project must be done using conventional over coring of the package.
- Methods used here for disassembling of the package and sectioning of the individual blocks were appropriate and can be used also in the future work.
- Methods for analyses were also appropriate but in the future also complementary methods should be used.
- Release of trace elements from the cement specimens was very limited and clear evidence for release from the cement specimens and bentonite diffusion was only found for Cs. For the other elements the levels found in the bentonite were close to or below the detection limit of the method or similar to the background levels in the different types of bentonite.
- Studies of cement/bentonite interactions showed that the Ca- and Mg-concentration in the bentonite had increased somewhat up to 5 and 3 mm respectively from the cement/bentonite interface for standard cement specimens. For low-pH specimens, the levels were lower and the affected volume smaller. In many of the specimens also increased levels of carbon was found which led to the conclusion that the whitish crust found at the interface consisted of $CaCO_3$ and $MgCO_3$.

References

SKB's (Svensk Kärnbränslehantering AB) publications can be found at www.skb.com/publications.

Cronstrand P, 2007. Modelling the long-time stability of the engineered barriers of SFR with respect to climate changes. SKB R-07-51, Svensk Kärnbränslehantering AB.

Cronstrand P, 2016. Long-term performance of the bentonite barrier in the SFR silo. SKB TR-15-08, Svensk Kärnbränslehantering AB.

Elfwing M, Evins L Z, Gontier M, Grahm P, Mårtensson P, Tunbrant S, 2013. SFL Concept study. Main report. SKB TR-13-14, Svensk Kärnbränslehantering AB.

Gaucher E, Tournassat C, Nowak C, 2005. Modelling the geochemical evolution of the multi-barrier system of the Silo of the SFR repository. Final report. SKB R-05-80, Svensk Kärnbränslehantering AB.

Höglund L-O, 2001. Project SAFE. Modelling the long-term concrete degradation processes in the Swedish SFR repository. SKB R-01-08, Svensk Kärnbränslehantering AB.

Höglund L-O, 2014. The impact on concrete degradation on BMA barrier functions. SKB R-13-40, Svensk Kärnbränslehantering AB.

Idiart A, Laviña M, 2019. Modelling of concrete degradation in a one-million-year perspective – Hydro-chemical processes. Report for the Safety evaluation SE-SFL. SKB R-19-13, Svensk Kärnbränslehantering AB.

Idiart A, Shafei B, 2019. Modelling of concrete degradation – Hydro-chemical processes. Report for the Safety evaluation SE-SFL. SKB R-19-11, Svensk Kärnbränslehantering AB.

Mårtensson P, 2015. Äspö Hard rock Laboratory. Concrete and Clay. Installation report. SKB P-15-01, Svensk Kärnbränslehantering AB.

SKB, 2015. Safety analysis for SFR. Long-term safety. Main report for the safety assessment SR-PSU. Revised edition. SKB TR-14-01, Svensk Kärnbränslehantering AB.

Svensson D, Dueck A, Nilsson U, Olsson S, Sandén T, Lydmark S, Jägervall S, Pedersen K, Hansen S, 2011. Alternative buffer material. Status of the ongoing laboratory investigation of reference materials and test package 1. SKB TR-11-06, Svensk Kärnbränslehantering AB.

Appendix A

Specimen names after sectioning of the package

Table A1. Specimen names after sectioning the package.

Specimen	Block #	Bentonite block	Specimen	Depth below rock floor (mm)	Position of the specimen in the bentonite block
FXM000685	CC20_01	FEB_01	CEMFE_40	1 000	NORTH
FXM000686	CC20_01	FEB_01	CEMFE_36	1 000	SOUTH
FXM000687	CC20_01	FEB_01	CEMMO_21	1 000	EAST
FXM000688	CC20_01	FEB_01	CEMMO_09	1 000	WEST
FXM000689	CC20_02	FEB_05	CEMCR_12	1 100	NORTH
FXM000690	CC20_02	FEB_05	CEMCR_17	1 100	SOUTH
FXM000691	CC20_02	FEB_05	CEMNI_20	1 100	EAST
FXM000692	CC20_02	FEB_05	CEMNI_24	1 100	WEST
FXM000693	CC20_03	FEB_08	SS_13	1 200	NORTH
FXM000694	CC20_03	FEB_08	SS_27	1 200	SOUTH
FXM000695	CC20_03	FEB_08	CS_27	1 200	EAST
FXM000696	CC20_03	FEB_08	CS_30	1 200	WEST
FXM000697	CC20_04	FEB_02	CEMSR_27	1 300	NORTH
FXM000698	CC20_04	FEB_02	CEMSR_21	1 300	SOUTH
FXM000699	CC20_04	FEB_02	CEM_24	1 300	EAST
FXM000700	CC20_04	FEB_02	CEM_29	1 300	WEST
FXM000701	CC20_05	FEB_06	CEMEU_06	1 400	NORTH
FXM000702	CC20_05	FEB_06	CEMEU_27	1 400	SOUTH
FXM000703	CC20_05	FEB_06	CEMCS_16	1 400	EAST
FXM000704	CC20_05	FEB_06	CEMCS_22	1 400	WEST
FXM000705	CC20_06	FEB_04	LOWFE_06	1 500	NORTH
FXM000706	CC20_06	FEB_04	LOWFE_03	1 500	SOUTH
FXM000707	CC20_06	FEB_04	LOWMO_03	1 500	EAST
FXM000708	CC20_06	FEB_04	LOWMO_13	1 500	WEST
FXM000709	CC20_07	FEB_07	LOWCR_11	1 600	NORTH
FXM000710	CC20_07	FEB_07	LOWCR_17	1 600	SOUTH
FXM000711	CC20_07	FEB_07	LOWNI_12	1 600	EAST
FXM000712	CC20_07	FEB_07	LOWNI_24	1 600	WEST
FXM000713	CC20_08	IBE_14	CEMFE_13	1 700	NORTH
FXM000714	CC20_08	IBE_14	CEMFE_28	1 700	SOUTH
FXM000715	CC20_08	IBE_14	CEMMO_16	1 700	EAST
FXM000716	CC20_08	IBE_14	CEMMO_05	1 700	WEST
FXM000717	CC20_09	IBE_15	CEMCR_25	1 800	NORTH
FXM000718	CC20_09	IBE_15	CEMCR_10	1 800	SOUTH
FXM000719	CC20_09	IBE_15	CEMNI_03	1 800	EAST
FXM000720	CC20_09	IBE_15	CEMNI_22	1 800	WEST
FXM000721	CC20_10	IBE_16	SS_15	1 900	NORTH
FXM000722	CC20_10	IBE_16	SS_37	1 900	SOUTH
FXM000723	CC20_10	IBE_16	CS_35	1 900	EAST
FXM000724	CC20_10	IBE_16	CS_24	1 900	WEST
FXM000725	CC20_11	IBE_12	CEMSR_16	2 000	NORTH
FXM000726	CC20_11	IBE_12	CEMSR_01	2 000	SOUTH
FXM000727	CC20_11	IBE_12	CEM_17	2 000	EAST
FXM000728	CC20_11	IBE_12	CEM_25	2 000	WEST
FXM000729	CC20_12	IBE_13	CEMEU_30	2 100	NORTH
FXM000730	CC20_12	IBE_13	CEMEU_12	2 100	SOUTH
FXM000731	CC20_12	IBE_13	CEMCS_22	2 100	EAST
FXM000732	CC20_12	IBE_13	CEMCS_24	2 100	WEST
FXM000733	CC20_13	IBE_09	LOWFE_16	2 200	NORTH

Specimen	Block #	Bentonite block	Specimen	Depth below rock floor (mm)	Position of the specimen in the bentonite block
FXM000734	CC20_13	IBE_09	LOWFE_23	2 200	SOUTH
FXM000735	CC20_13	IBE_09	LOWMO_26	2 200	EAST
FXM000736	CC20_13	IBE_09	LOWMO_25	2 200	WEST
FXM000737	CC20_14	IBE_10	LOWCR_07	2 300	NORTH
FXM000738	CC20_14	IBE_10	LOWCR_20	2 300	SOUTH
FXM000739	CC20_14	IBE_10	LOWNI_08	2 300	EAST
FXM000740	CC20_14	IBE_10	LOWNI_27	2 300	WEST
FXM000741	CC20_15	WYO_25	-	2 400	NORTH
FXM000742	CC20_15	WYO_25	-	2 400	SOUTH
FXM000743	CC20_15	WYO_25	-	2 400	EAST
FXM000744	CC20_15	WYO_25	-	2 400	WEST
FXM000745	CC20_16	WYO_28	CEMFE_04	2 500	NORTH
FXM000746	CC20_16	WYO_28	CEMFE_17	2 500	SOUTH
FXM000747	CC20_16	WYO_28	CEMMO_30	2 500	EAST
FXM000748	CC20_16	WYO_28	CEMMO_02	2 500	WEST
FXM000749	CC20_17	WYO_23	CEMCR_22	2 600	NORTH
FXM000750	CC20_17	WYO_23	CEMCR_24	2 600	SOUTH
FXM000751	CC20_17	WYO_23	CEMNI_15	2 600	EAST
FXM000752	CC20_17	WYO_23	CEMNI_27	2 600	WEST
FXM000753	CC20_18	WYO_14	SS_04	2 700	NORTH
FXM000754	CC20_18	WYO_14	SS_05	2 700	SOUTH
FXM000755	CC20_18	WYO_14	CS_08	2 700	EAST
FXM000756	CC20_18	WYO_14	CS_02	2 700	WEST
FXM000757	CC20_19	WYO_12	CEMSR_06	2 800	NORTH
FXM000758	CC20_19	WYO_12	CEMSR_14	2 800	SOUTH
FXM000759	CC20_19	WYO_12	CEM_31	2 800	EAST
FXM000760	CC20_19	WYO_12	CEM_23	2 800	WEST
FXM000761	CC20_20	WYO_10	CEMEU_08	2 900	NORTH
FXM000762	CC20_20	WYO_10	CEMEU_14	2 900	SOUTH
FXM000763	CC20_20	WYO_10	CEMCS_20	2 900	EAST
FXM000764	CC20_20	WYO_10	CEMCS_10	2 900	WEST
FXM000765	CC20_21	WYO_24	LOWFE_17	3 000	NORTH
FXM000766	CC20_21	WYO_24	LOWFE_05	3 000	SOUTH
FXM000767	CC20_21	WYO_24	LOWMO_31	3 000	EAST
FXM000768	CC20_21	WYO_24	LOWMO_16	3 000	WEST
FXM000769	CC20_22	WYO_22	LOWCR_01	3 100	NORTH
FXM000770	CC20_22	WYO_22	LOWCR_05	3 100	SOUTH
FXM000771	CC20_22	WYO_22	LOWNI_16	3 100	EAST
FXM000772	CC20_22	WYO_22	LOWNI_18	3 100	WEST
FXM000773	CC20_23	WYO_19	-	3 200	NORTH
FXM000774	CC20_23	WYO_19	-	3 200	SOUTH
FXM000775	CC20_23	WYO_19	-	3 200	EAST
FXM000776	CC20_23	WYO_19	-	3 200	WEST
FXM000777	CC20_24	ASH_11	CEMFE_34	3 300	NORTH
FXM000778	CC20_24	ASH_11	CEMFE_33	3 300	SOUTH
FXM000779	CC20_24	ASH_11	CEMMO_15	3 300	EAST
FXM000780	CC20_24	ASH_11	CEMMO_07	3 300	WEST
FXM000781	CC20_25	ASH_39	CEMCR_09	3 400	NORTH
FXM000782	CC20_25	ASH_39	CEMCR_08	3 400	SOUTH
FXM000783	CC20_25	ASH_39	CEMNI_17	3 400	EAST
FXM000784	CC20_25	ASH_39	CEMNI_26	3 400	WEST
FXM000785	CC20_26	ASH_09	SS_28	3 500	NORTH
FXM000786	CC20_26	ASH_09	SS_25	3 500	SOUTH
FXM000787	CC20_26	ASH_09	CS_19	3 500	EAST
FXM000788	CC20_26	ASH_09	CS_26	3 500	WEST

Specimen	Block #	Bentonite block	Specimen	Depth below rock floor (mm)	Position of the specimen in the bentonite block
FXM000789	CC20_27	ASH_26	CEMSR_23	3 600	NORTH
FXM000790	CC20_27	ASH_26	CEMSR_19	3 600	SOUTH
FXM000791	CC20_27	ASH_26	CEM_10	3 600	EAST
FXM000792	CC20_27	ASH_26	CEM_04	3 600	WEST
FXM000793	CC20_28	ASH_07	CEMEU_29	3 700	NORTH
FXM000794	CC20_28	ASH_07	CEMEU_19	3 700	SOUTH
FXM000795	CC20_28	ASH_07	CEMCS_19	3 700	EAST
FXM000796	CC20_28	ASH_07	CEMCS_01	3 700	WEST
FXM000797	CC20_29	ASH_06	LOWFE_21	3 800	NORTH
FXM000798	CC20_29	ASH_06	LOWFE_20	3 800	SOUTH
FXM000799	CC20_29	ASH_06	LOWMO_21	3 800	EAST
FXM000800	CC20_29	ASH_06	LOWMO_15	3 800	WEST
FXM000801	CC20_30	ASH_04	LOWCR_27	3 900	NORTH
FXM000802	CC20_30	ASH_04	LOWCR_09	3 900	SOUTH
FXM000803	CC20_30	ASH_04	LOWNI_01	3 900	EAST
FXM000804	CC20_30	ASH_04	LOWNI_23	3 900	WEST

Arkitektkopia AB, Bromma, 2019

SKB is responsible for managing spent nuclear fuel and radioactive waste produced by the Swedish nuclear power plants such that man and the environment are protected in the near and distant future.

skb.se